

# Synthesis and Characterization of $[M^{III}(PS)_2(L)]$ Mixed-Ligand Compounds ( $M = \text{Re}, {}^{99}\text{Tc}$ ; PS = Phosphinothiolate; L = Dithiocarbamate) as Potential Models for the Development of New Agents for SPECT Imaging and Radiotherapy

N. Salvatore,<sup>\*,†</sup> N. Morellato,<sup>†</sup> A. Venzo,<sup>‡</sup> F. Refosco,<sup>§</sup> A. Dolmella,<sup>†</sup> and C. Bolzati<sup>\*,§</sup>

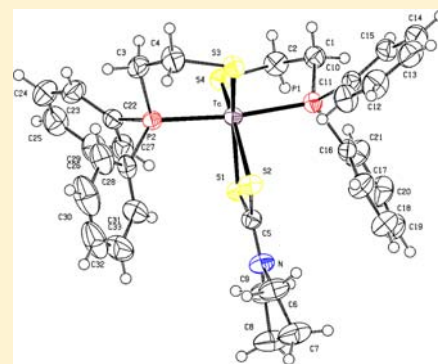
<sup>†</sup>Dipartimento di Scienze del Farmaco, Università di Padova, Via Marzolo 5, 35131 Padova, Italy

<sup>‡</sup>ISTM-CNR, Via Marzolo 1, 35131 Padova, Italy

<sup>§</sup>ICIS-CNR, Corso Stati Uniti, 4, 35127 Padova, Italy

## S Supporting Information

**ABSTRACT:** The synthesis and characterization of a new series of neutral, six-coordinated mixed-ligand compounds  $[M^{III}(PS)_2(L)]$  ( $M = \text{Re}; {}^{99}\text{Tc}$ ), where PS is bis(arylalkyl)- or trialkylphosphinothiolate and L is dithiocarbamate, are reported. Stable  $[M^{III}(PS)_2(L)]$  complexes were easily synthesized, in good yield, starting from precursors where the metal was in different oxidation states (III, V, and VII), involving ligand-exchange and/or redox-substitution reactions. The compounds were characterized by elemental analysis, positive-ion electrospray ionization mass spectrometry, multinuclear NMR spectroscopy, cyclic voltammetry, and X-ray diffraction analysis. All complexes are constituted by the presence of the  $[M^{III}(PS)_2]^+$  moiety, where two phosphinothiolate ligands are tightly bound to the metal and the remaining two positions are saturated by a dithiocarbamate chelate, also carrying bulky bioactive molecules [e.g., (2-methoxyphenyl)-piperazine]. X-ray analyses were performed on crystalline specimens of four different Re/ ${}^{99}\text{Tc}$  compounds sharing a distorted trigonal-prismatic geometry, with a  $P_2S_4$  coordination donor set. The possibility of easily preparing these  $[M^{III}(PS)_2(L)]$  complexes, starting from the corresponding permetalate anions, in mild reaction conditions and in high yield, lays the first stone to the preparation of a new series of  $M^{III}$ -based ( $M = {}^{99}\text{Tc}/{}^{188}\text{Re}$ ) compounds potentially useful in theragnostic applications.



## INTRODUCTION

Inorganic and organometallic chemistry have always played key roles in the development of metal-based radiopharmaceuticals. Among the different radiometals exploited in nuclear medicine (NM),  ${}^{99m}\text{Tc}$  (6.02 h half-life, 140 keV  $\gamma$  radiation) and  ${}^{188}\text{Re}$  (17 h half-life, 2.12 MeV  $\beta^-$  max radiation) represent an attractive pair of radionuclides. The combination of their nuclear, physical, and chemical properties, together with  ${}^{99m}\text{Tc}/{}^{188}\text{Re}$  onsite availability (thanks to corresponding  ${}^{99}\text{Mo}/{}^{99m}\text{Tc}$  and  ${}^{188}\text{W}/{}^{188}\text{Re}$  generator systems), makes these two congeners good candidates for the development of matched-pair agents useful in theragnostic applications.<sup>1,2</sup>

With respect to the matching-pair theory, there is a close analogy between technetium and rhenium, making the chemistry of the two elements the same or virtually identical in many cases. In vivo studies, carried out on  ${}^{99m}\text{Tc}/{}^{188}\text{Re}$  homologues, have established that a pair of technetium and rhenium compounds having exactly the same molecular geometry and ligand composition always exhibits the same biodistribution pattern, to indicate that a  ${}^{99m}\text{Tc}$  complex can be conveniently employed to determine the biological properties

of the corresponding rhenium analogue. This occurrence is important for NM applications and offers the possibility of developing  ${}^{99m}\text{Tc}$  agents useful as the “matched pair” of the corresponding  ${}^{188}\text{Re}$  agents, making it feasible to obtain excellent diagnostic imaging in patients and allowing a pre- and postassessment of patients treated with therapeutic  ${}^{188}\text{Re}$  analogues.<sup>1</sup> Likewise, according to this, the “matched-pair” theory can also be expanded to the use of a *cold* rhenium compound as a cytotoxic or cytostatic agent. The possibility of labeling this compound with  ${}^{99m}\text{Tc}$  realizes a matched pair by taking *cold* rhenium for therapy and *hot* technetium for diagnosis.<sup>2</sup>

Considering the current  ${}^{99m}\text{Tc}/{}^{188}\text{Re}$  radiopharmaceutical scenario, it appears that, while  ${}^{99m}\text{Tc}$  continues to be the first choice radionuclide in SPECT imaging (it is indispensable for an estimated 70000 medical imaging procedures that take place daily around the world), the use of  ${}^{188}\text{Re}$ -based compounds as therapeutic agents still remains limited, so that it is difficult to predict whether the  ${}^{188}\text{Re}$  radiopharmaceuticals will make their

Received: January 15, 2013

Published: May 21, 2013

way into the market.<sup>1</sup> Therefore, efforts addressed at devising new strategies aimed at finding efficient new  $^{99m}\text{Tc}/^{188}\text{Re}$ -based agents are justified.

The trivalent state is one of the most common and stable oxidation states of both technetium and rhenium. In spite of this, none of the radiopharmaceuticals currently in clinical use contains the metal in this oxidation state and only a limited number of studies involving the use of  $\text{M}^{\text{III}}(^{99m}\text{Tc}/^{188}\text{Re})$  are reported. Nevertheless, examples of  $^{99m}\text{Tc}^{\text{III}}$ -based radiopharmaceuticals have already been described in the past years, with one remarkable example being  $^{99m}\text{Tc}$ -terboroxime, Cardiotec, approved by the Food and Drug Administration as a myocardial imaging agent.

A common reason to explain the low number of  $\text{M}^{\text{III}}$  complexes produced at the tracer level takes into account the lack of easily accessible methods for preparing these compounds in aqueous solutions. This occurrence is probably due to the fact that at the millimolar level the preparations of such compounds are carried out in organic solvents, using labile prerduced  $\text{M}^{\text{III}/\text{IV}}$  complexes as starting materials, in the presence of a slight excess of equimolar amounts of ligands and, consequently, in reaction conditions not directly applicable to the production of the same complex at the micromolar level. At the tracer level, indeed, permethylate anions, in the form of  $\text{NaMO}_4$  ( $\text{M} = ^{99m}\text{Tc}/^{188}\text{Re}$ ), are used as starting materials and sterile and pyrogen-free physiological conditions are required for *in vivo* applications. Therefore, the chemistry of  $\text{Tc}^{\text{III}}$  and  $\text{Re}^{\text{III}}$  complexes as applied to NM can still be considered as largely unexplored.

As a matter of fact, the literature reports a relatively rich chemistry related to the synthesis of  $\text{Tc}^{\text{III}}$  and  $\text{Re}^{\text{III}}$  complexes in macroscopic amounts.<sup>3–6</sup> In the trivalent state, technetium and rhenium exhibit a  $d^4$  electronic configuration combined with a trigonal-bipyramidal or an octahedral geometry or, more rarely, with a distorted trigonal-prismatic arrangement. In these complexes, the most represented donor atom is sulfur, often accompanied by other atoms such as phosphorus, less frequently nitrogen or oxygen, and only occasionally by sulfur.<sup>6</sup> In this connection,  $[\text{M}(\text{R-PhCS}_3)_2(\text{R-PhCS}_2)]$  and  $[\text{M}(\text{R-PhCS}_3)_2(\text{Et}_2\text{NCS}_2)]$  complexes constitute two rare examples of a “sulfur-rich”  $\text{S}_6$  coordination environment.<sup>7</sup> Interestingly, these  $\text{S}_6$  complexes are closely similar, from structural and electronic points of view, to other trisubstituted  $\text{M}^{\text{III}}$  complexes, of the general formulas  $\{\text{Tc}[(\text{Ph})_2\text{PC}_6\text{H}_4\text{S}]\}_3$ <sup>8</sup> and  $\{\text{Tc}[\text{Ph}_2\text{P}(\text{C}_6\text{H}_4\text{NH}_2\text{-}o)]_2[\text{Ph}_2\text{P}(\text{C}_6\text{H}_4\text{NH}_2\text{-}o)]\}^+$ ,<sup>9</sup> despite the differences in the coordination spheres ( $\text{S}_6$  vs  $\text{P}_3\text{S}_3$  and  $\text{P}_3\text{N}_3$ ).

All of these compounds, sketched in Figure 1 using an octahedral description, are characterized by two identical ligands that provide two apical trans-positioned  $\pi$ -acceptor atoms ( $\text{S}_{\text{thiourea}}$  in A or P in B and C) connected with two strong cis-positioned  $\pi$ -donor atoms ( $\text{S}_{\text{thiolate}}$  and N) and a third ligand with chemical and/or electronic properties different from those of the two other ligands.

Evaluation of the bond distances, from the X-ray crystal structure data of A–C, clearly shows that in these compounds the two apical trans-positioned  $\pi$ -acceptor atoms and the two cis-positioned  $\pi$ -donor atoms are tightly bonded to the metal center defining a stable  $[\text{M}(\text{PhS}_3)_2]^+$ ,  $[\text{M}(\text{PS})_2]^+$  or  $[\text{M}(\text{PNH})_2]^+$  moiety, whereas the bond lengths of the third ligand ( $\text{S}^{\text{N}}\text{S}$ ;  $\text{P}^{\text{N}}\text{S}$ ;  $\text{P}^{\text{N}}\text{NH}_2$ ) due to the *labilizing effect* of the two strong cis-positioned  $\pi$ -donor atoms appear significantly longer with respect to those of the other ligands in the coordination sphere.<sup>7,8</sup> Such an *effect* is particularly self-evident in another

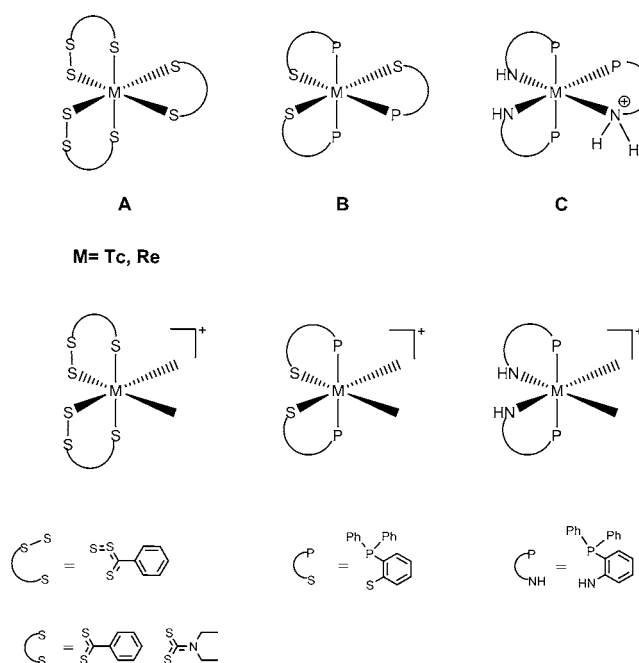


**Figure 1.** Schematic drawing of six-coordinated  $\text{M}^{\text{III}}$  complexes. The lengthened bidentate ligand is displayed on the right side of the molecules (up) and of the corresponding moiety (down). A is for the  $[\text{M}(\text{R-PhCS}_3)_2(\text{R-PhCS}_2)]$  and  $[\text{M}(\text{R-PhCS}_3)_2(\text{Et}_2\text{NCS}_2)]$  complexes, B is for the  $\{\text{Tc}[(\text{Ph})_2\text{PC}_6\text{H}_4\text{S}]\}_3$  complex, and C is for the  $[\text{Tc}\{\text{Ph}_2\text{P}(\text{C}_6\text{H}_4\text{NH}_2\text{-}o)\}_2\{\text{Ph}_2\text{P}(\text{C}_6\text{H}_4\text{NH}_2\text{-}o)\}^+$  complex.

class of related complexes, of the type  $[\text{Tc}(\text{PS})_2(\text{S}^{\text{N}}\text{P}=\text{O})]^{10}$  and  $[\text{Re}(\text{PS})_2(\text{S}^{\text{N}}\text{P})]^{11}$  also containing the  $[\text{M}^{\text{III}}(\text{PS})_2]^+$  moiety, where replacement of triarylphosphinothiolate, in B-like compounds, with bis(arylalkyl)phosphinothiolate ligands, which precludes  $\pi$ -electronic conjugation, gives rise to trigonal-bipyramidal arrangements with two  $\pi$ -acceptor atoms (P) at the apexes and three  $\pi$ -donor atoms (S) at the base of the pyramid.

Instead, for the complexes described in Figure 1, six-coordination appears guaranteed by the presence of a ligand capable of delocalizing the electron density via  $\pi$  orbitals such as dithiobenzoate/dithiocarbamate in A and aromatic phosphinothiolate and phosphinoamine in B and C. It follows that, in these  $\text{M}^{\text{III}}$  complexes, if the  $\pi$  conjugation is precluded, then the particular combination of  $\pi$ -acceptor and  $\pi$ -donor atoms drives the system toward five-coordination.<sup>7a</sup>

Accordingly, it should be possible to design six-coordinated mixed-ligand  $\text{M}^{\text{III}}$  compounds, characterized by the presence of two identical bidentate ligands containing a neutral  $\pi$ -acceptor atom and a negatively charged  $\pi$ -donor atom and a third different bidentate ligand capable of delocalizing via  $\pi$  orbitals the high electron density thus allowing the complex to expand the coordination sphere toward six-coordination.

In our ongoing efforts to investigate the coordination chemistry of  $^{99m}\text{Tc}$  and  $\text{Re}$  with phosphinothiolate and dithiocarbamate ligands, we devised a novel class of mixed-ligand complexes characterized by the  $[\text{M}^{\text{III}}(\text{PS})_2]^+$  moiety, where the two empty positions of a six-coordinate environment are saturated by one  $\pi$ -conjugated dithiocarbamate ligand.

It should be noted that the literature describes a unique example of such types of compounds, the synthesis and characterization of the  $\{\text{Re}[\text{Ph}_2\text{P}(\text{C}_6\text{H}_4\text{S-}o)]_2(\text{S}_2\text{CN-Et}_2)\}\cdot\text{Me}_2\text{CO}$  complex.<sup>12</sup>

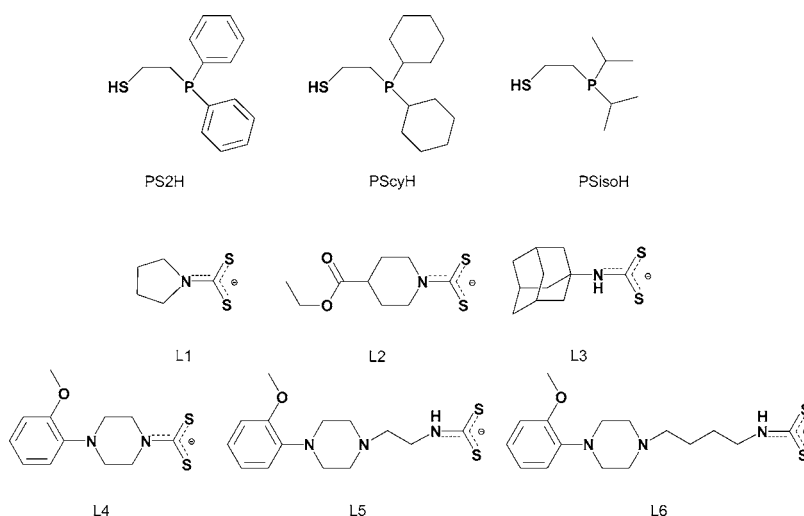


**Figure 2.** Phosphinothiol and dithiocarbamate ligands used in our experiments.

This study describes the synthesis and the solution and solid-state characterization of the molecular structure of a series of  $^{99}\text{Tc}$  and Re compounds of the type  $[\text{M}^{\text{III}}(\text{PS})_2(\text{L})]$ , where PS and L indicate the phosphinothiolate and dithiocarbamate ligands, respectively.

The phosphinothiols (PSH) and dithiocarbamates (L) used in our experiments are shown in Figure 2.

## EXPERIMENTAL SECTION

**Materials.** All chemicals and reagents, as well as ammonium pyrrolidinedithiocarbamate ( $\text{NH}_4\text{L1}$ ) and  $[\text{NBu}_4][\text{ReO}_4]$ , were purchased from Aldrich Chemicals (Milano, Italy). The solvents were reagent grade and were used without further purification.

2-(Diphenylphosphino)ethanethiol (PS2H), 2-(dicyclohexylphosphino)ethanethiol (PScyH), and 2-(diisopropylphosphino)ethanethiol (PSisoH) were purchased from Argus Chemicals (Prato, Italy).

Commercially available  $[\text{NH}_4][^{99}\text{TcO}_4]$  (Oak Ridge National Laboratories) was purified from a black contaminant ( $^{99}\text{TcO}_2 \cdot n\text{H}_2\text{O}$ ) by the addition of  $\text{H}_2\text{O}_2$  and  $\text{NH}_4\text{OH}$ . When a clear solution was obtained, the mixture was boiled to destroy the residual peroxide and an excess of  $\text{NBu}_4\text{Br}$  in water was added.

Dinuclear  $\mu$ -oxorhenium(V) complexes,  $[\text{Re}^{\text{V}}_2\text{O}_3(\text{L})_4]$  (L = L1–L4), were prepared as previously described by Rowbottom and Wilkinson.<sup>13</sup> The synthesis and characterization data for these compounds are reported in the Supporting Information.

$[\text{Re}^{\text{III}}\text{Cl}_3(\text{MeCN})(\text{PPh}_3)_2]$ ,  $[\text{Re}^{\text{V}}(\text{O})\text{Cl}_3(\text{PPh}_3)_2]$ , and  $[\text{Re}^{\text{III}}\text{Cl}_3(\text{MeCN})(\text{PPh}_3)_2]$  were prepared according to literature methods.<sup>14</sup>

Sodium 4-(2-methoxyphenyl)piperazine-1-dithiocarbamate (NaL4), sodium 2-[4-(2-methoxyphenyl)piperazin-1-yl]ethylthiocarbamate (NaL5), and sodium 4-[4-(2-methoxyphenyl)piperazin-1-yl]butylthiocarbamate (NaL6) were prepared as previously described.<sup>15</sup> The synthesis and characterization of the 4-(ethoxycarbonyl)piperidinedithiocarbamate, 4-(ethoxycarbonyl)piperidinium salt ( $\text{EtOOCpIP2}$ ), and sodium N-adamantylthiocarbamate (NaL3) ligands are reported in the Supporting Information.

**Physical Measurements.** Elemental analyses (C, H, N, and S) were performed on a Perkin-Elmer model 240B elemental analyzer.  $^1\text{H}$ ,  $^{13}\text{C}$ , and  $^{31}\text{P}$  NMR spectra of the complexes were acquired at room temperature on a Bruker AMX 300 or a Bruker AMX 400 instrument, using  $\text{SiMe}_4$  as the internal reference ( $^1\text{H}$  and  $^{13}\text{C}$ ) and 85% aqueous  $\text{H}_3\text{PO}_4$  as the external reference ( $^{31}\text{P}$ ).

Mass spectrometric measurements (electrospray ionization mass spectrometry, ESI-MS) were performed with an ESI time-of-flight

Mariner biospectrometry workstation (PerSeptive Biosystems, Stamford, TX).

Cyclic voltammetry measurements were performed on a BAS (Bioanalytical System Inc.) CV-1B cyclic voltammograph at 293 K under an atmosphere of dinitrogen, in anhydrous deoxygenated dichloromethane solutions ( $3.5 \times 10^{-3}$  M) with  $[\text{NBu}_4][\text{ClO}_4]$  (0.1 M) as the supporting electrolyte, by using a conventional three-electrode cell, recording at  $0.2 \text{ V s}^{-1}$ . A platinum disk (area ca.  $1.28 \text{ mm}^2$ ) was used as the working electrode, a platinum wire as the counter electrode, and a silver wire as the quasi-reference electrode. Controlled-potential coulometries were performed using an Amel model 721 integrator, in an H-shaped cell containing, in arm 1, a platinum gauze working electrode and an  $\text{Ag}/\text{Ag}^+$  reference electrode isolated inside a salt bridge by a medium-glass frit and, in arm 2, an auxiliary platinum-foil electrode. All potentials were internally referred against the ferrocene couple ( $400 \text{ mV}$  vs NHE).

Dry column flash chromatography purifications were accomplished on a  $\text{SiO}_2$  column ( $4 \text{ cm} \times 2 \text{ cm}$ ; grade 9385 pore size  $60 \text{ \AA}$ ; 230–400 mesh particles).

Thin-layer chromatography (TLC) analyses were carried out on  $\text{SiO}_2 \text{ F}_{254\text{S}}$  plates (Merck) using dichloromethane or dichloromethane/methanol (9:1) as the mobile phase. The  $^{99}\text{Tc}$  radioactivity on TLC plates was detected and measured by means of a Cyclone Instrument equipped with a phosphorus imaging screen and OptiQuant image analysis software (Packard, Meridian, CT).

**Caution!**  $^{99}\text{Tc}$  is a weak  $\beta$  emitter ( $E_\beta = 0.292 \text{ mV}$ ;  $t_{1/2} = 1.12 \times 10^5$  years). All manipulations were carried out in laboratories approved for low-level radioactivity use. Handling milligram amounts of  $^{99}\text{Tc}$  does not present a serious health hazard because common laboratory glassware provides adequate shielding and all work is performed in approved and monitored hoods and gloveboxes. Bremsstrahlung is not a significant problem because of the low energy of the  $\beta$  particles; however, proper radiation safety procedures must be followed at all times, and particular care should be taken when handling solid samples.

**General note:** because of the tendency of the phosphinothiol ligands to oxidize, all of the solvents used in the reactions with PSH were previously degassed to remove dissolved trace dioxygen.

All reactions and manipulations were performed under a dinitrogen atmosphere using standard Schlenk techniques.

TLC and ESI(+)-MS analyses of the reaction mixtures indicated the quantitative conversion of the starting compound into the final  $[\text{M}(\text{PS})_2(\text{L})]$  complex. Thus, the decrease in the final yields of the products was essentially due to the purification procedure.

**Synthesis of the  $[\text{Re}(\text{PS})_2(\text{L})]$  Complexes (1–8; PS = PS2, PScy, PSiso; L = L1–L6).** Different procedures were applied for  $[\text{Re}^{\text{III}}(\text{PS})_2(\text{L})]$  preparation; methods change with the starting material.

**Method A.** (i) To an orange suspension of  $[\text{ReCl}_3(\text{MeCN})(\text{PPh}_3)_2]$  (13.9 mg, 0.016 mmol) in toluene (1.5 mL) was added the selected PS ligand (0.048 mmol), dissolved in 1 mL of ethanol, rapidly followed by the dithiocarbamate ligand (L; 0.080 mmol whenever PSH = PS2H and 0.040 mmol whenever PSH = PScyH or PSisoH). The mixture was stirred at reflux for 1 h, during which the solution became clear and the color changed to bright green. The solvents were removed by a gentle dinitrogen stream, and a bright-green residue was obtained. This was dissolved in dichloromethane (3 mL), filtered, and extracted with water ( $3 \times 3$  mL) to remove excess Ln ligand. The organic phase was collected and dried with anhydrous  $\text{Na}_2\text{SO}_4$ , and the solvent was evaporated, giving a crude product, which was purified by dry column flash chromatography as described below.

(ii) Alternatively, a two-step procedure was used. To the initial orange suspension was added the PS ligand, and the resulting mixture was stirred at reflux for 30 min, during which it became dark brown. Then the Ln ligand was added, and the reaction mixture rapidly became clear and the color change to bright green.

**Method B.** (iii) This method was used only for selected  $\text{Re}^{\text{III}}$  complexes (1–4). To a yellow-to-dark-brown suspension of  $[\text{Re}_2\text{O}_3(\text{L})_4]$  (0.008 mmol) in acetone (5 mL) or alternatively in toluene/ethanol (1.5/3.5 mL) was added the selected PS2H ligand (0.048 mmol/1 mL of acetone or ethanol). The resulting mixture was stirred to reflux for 12 h, during which it became green-brown. The solvents were removed by a gentle dinitrogen stream, and the residue was treated as indicated above (method A).

**Method C.** (iv) To an olive-green suspension of  $[\text{Re}(\text{O})\text{Cl}_3(\text{PPh}_3)_2]$  (11.6 mg, 0.014 mmol) in toluene (1.5 mL) was rapidly added the selected PSH ligand (0.049 mmol), dissolved in 1 mL of ethanol, followed by the Ln ligand (0.070 mmol whenever PSH = PS2H and 0.035 mmol whenever PSH = PScyH or PSisoH), dissolved in 3 mL of ethanol. The resulting mixture was stirred to reflux for 1 h, during which it became progressively clear and bright green.

The solvents were removed by a gentle dinitrogen stream, and the residue was treated as indicated above (method A).

**Method D.** (v) To an ethanol solution (0.5 mL) containing  $[\text{NBu}_4][\text{ReO}_4]$  (6.9 mg, 0.014 mmol) and triphenylphosphine (14.6 mg, 0.056 mmol) was added an excess of  $\text{HCl}_{\text{conc}}$  (0.03 mL). The reaction mixture was stirred at reflux for 1 h to obtain an olive-green solution ( $[\text{Re}(\text{O})\text{Cl}_3(\text{PPh}_3)_2]$ ). The resulting mixture was allowed to cool to room temperature, and the reaction pH was adjusted to 7.3 by the addition of triethylamine (0.05 mL). After this, the selected PSH ligand (0.049 mmol), dissolved in ethanol (1 mL), was rapidly added, followed by the Ln ligand (0.070 mmol whenever PSH = PS2H and 0.035 mmol whenever PSH = PScyH or PSisoH) dissolved in 3 mL of ethanol. The resulting mixture was stirred at reflux for 1 h, during which it became progressively clear and bright green. The solvents were removed by a gentle dinitrogen stream, and the residue was treated as indicated above (method A).

Column chromatography was necessary to obtain the pure rhenium complexes. Extreme care was taken for the purification of oxidizable complexes 7 and 8, performing the procedure under an inert dinitrogen atmosphere.

All rhenium complexes were soluble in chlorinated solvents and dimethyl sulfoxide (DMSO), slightly soluble in methanol, *n*-hexane, and diethyl ether, and insoluble in water.

**$[\text{Re}(\text{PS}_2)_2(\text{L}1)]$  (1).** The crude product was dissolved in the mixture *n*-hexane/dichloromethane (1:1; 1 mL), loaded onto a  $\text{SiO}_2$  column set for dry column flash chromatography, and eluted with *n*-hexane/dichloromethane (1:1; 5 mL  $\times$  2) and dichloromethane (5 mL  $\times$  3). A bright-green band was separated and collected. The eluate was evaporated to yield the pure compound 1. Yield: 71% (methods A, C, and D); 62% (method B). Elem anal. Calcd for  $\text{C}_{33}\text{H}_{36}\text{NP}_2\text{ReS}_4$  (MW = 823.06): C, 48.16; H, 4.41; N, 1.70. Found: C, 47.33; H, 4.25; N, 1.93. ESI(+)-MS:  $m/z$  823.06 ( $\text{M}^+$ , 100%).  $^{31}\text{P}$  NMR (161.98 MHz,  $\text{CD}_2\text{Cl}_2$ ):  $\delta$  25.97 (s).  $^1\text{H}$  NMR (400 MHz,  $\text{CD}_2\text{Cl}_2$ ):  $\delta$  1.64 (m, 4H,  $\text{N}(\text{CH}_2\text{CH}_2)_2$ ); 2.38, 2.90 (2 m, 2H + 2H,  $\text{PCH}_2\text{CH}_2\text{S}$ ); 3.06, 3.52 (2 m, 2H + 2H,  $\text{PCH}_2\text{CH}_2\text{S}$ ); 3.30 (m, 4H,  $\text{N}(\text{CH}_2\text{CH}_2)_2$ ); 7.28 (m, 2H,  $\text{H}_{\text{arom}}$  p); 7.36 (m, 4H,  $\text{H}_{\text{arom}}$  m); 7.40 (m, 2H,  $\text{H}_{\text{arom}}$  p'); 7.41 (m, 4H,  $\text{H}_{\text{arom}}$  m'); 7.65 (m, 4H,  $\text{H}_{\text{arom}}$  o'); 7.67 (m, 4H,  $\text{H}_{\text{arom}}$  o).

(100 MHz  $\text{CD}_2\text{Cl}_2$ ):  $\delta$  25.14 (s,  $\text{N}(\text{CH}_2\text{CH}_2)_2$ ); 36.57 (m,  $\text{PCH}_2\text{CH}_2\text{S}$ ); 47.64 (s,  $\text{N}(\text{CH}_2\text{CH}_2)_2$ ); 56.09 (s,  $\text{PCH}_2\text{CH}_2\text{S}$ ); 127.32 (s,  $\text{C}_{\text{arom}}$  m'); 128.26 (s,  $\text{C}_{\text{arom}}$  m); 128.81 (s,  $\text{C}_{\text{arom}}$  p'); 129.69 (s,  $\text{C}_{\text{arom}}$  p); 132.87 (s,  $\text{C}_{\text{arom}}$  o'); 133.65 (s,  $\text{C}_{\text{arom}}$  o);  $\sim$ 137.69 (s,  $\text{C}_{\text{quat. arom}}$  P);  $\sim$ 139.55 (s,  $\text{C}_{\text{quat. arom}}$  P);  $\sim$ 197.30 ( $\text{CS}_2$ ). Note: signals marked with  $\sim$  are derived from the heteronuclear multiple-bond correlation (HMBC) analysis only.

**$[\text{Re}(\text{PS}_2)_2(\text{L}2)]$  (2).** The crude product was purified as described for compound 1. Yield: 77% (methods A, C, and D); 68% (method B). Elem anal. Calcd for  $\text{C}_{37}\text{H}_{42}\text{NO}_2\text{P}_2\text{ReS}_4$  (MW = 909.15): C, 48.88; H, 4.66; N, 1.54. Found: C, 48.86; H, 4.72; N, 1.52. ESI(+)-MS:  $m/z$  909.10 ( $\text{M}^+$ , 100%).  $^{31}\text{P}$  NMR (161.98 MHz,  $\text{CD}_2\text{Cl}_2$ ):  $\delta$  27.10 (s).  $^1\text{H}$  NMR (400 MHz,  $\text{CD}_2\text{Cl}_2$ ):  $\delta$  1.14 (m, 2H,  $\text{CH}_2(\text{axial})\text{CHC}(\text{O})\text{OEt}$ ); 1.28 (m, 3H,  $\text{C}(\text{O})\text{OCH}_2\text{CH}_3$ ); 1.60 (m, 2H,  $\text{CH}_2(\text{equatorial})\text{CHC}(\text{O})$ ); 2.31 (m, 1H,  $\text{CH}_2\text{CHC}(\text{O})\text{OEt}$ ); 2.31, 2.88 (2m, 2H + 2H,  $\text{PCH}_2\text{CH}_2\text{S}$ ); 2.67 (m, 2H,  $\text{S}_2\text{CNCH}_2(\text{axial})$ ); 3.02, 3.57 (2 m, 2H + 2H  $\text{PCH}_2\text{CH}_2\text{S}$ ); 3.94 (m, 2H,  $\text{S}_2\text{CNCH}_2(\text{equatorial})$ ); 4.15 (m, 2H,  $\text{C}(\text{O})\text{OCH}_2\text{CH}_3$ ); 7.28 (m, 2H,  $\text{H}_{\text{arom}}$  p); 7.35 (m, 4H,  $\text{H}_{\text{arom}}$  m); 7.40 (m, 2H,  $\text{H}_{\text{arom}}$  p'); 7.41 (m, 4H,  $\text{H}_{\text{arom}}$  m); 7.62 (m, 4H,  $\text{H}_{\text{arom}}$  o'); 7.64 (m, 4H,  $\text{H}_{\text{arom}}$  o).  $^{13}\text{C}$  NMR (100 MHz,  $\text{CD}_2\text{Cl}_2$ ):  $\delta$  13.98 (s,  $\text{C}(\text{O})\text{OCH}_2\text{CH}_3$ ); 27.11, 27.24 (2s,  $\text{CH}_2\text{CHC}(\text{O})\text{OEt}$ ); 36.18 (m,  $\text{PCH}_2\text{CH}_2\text{S}$ ); 40.16 (s,  $\text{CHC}(\text{O})\text{OEt}$ ); 43.19 (s,  $\text{S}_2\text{CNCH}_2$ ); 55.04 (s,  $\text{PCH}_2\text{CH}_2\text{S}$ ); 60.47 ( $\text{C}(\text{O})\text{OCH}_2\text{CH}_3$ ); 127.07 (s br,  $\text{C}_{\text{arom}}$  m'); 127.84 (s br,  $\text{C}_{\text{arom}}$  m); 128.46 (s br,  $\text{C}_{\text{arom}}$  p'); 129.29 (s br,  $\text{C}_{\text{arom}}$  p); 132.30 (s br,  $\text{C}_{\text{arom}}$  o'); 133.24 (s br,  $\text{C}_{\text{arom}}$  o),  $\sim$ 137.13,  $\sim$ 138.79,  $\sim$ 139.05 ( $\text{C}_{\text{quat. arom}}$  P); 173.52 (s,  $\text{C}=\text{O}$ );  $\sim$ 198.80 ( $\text{CS}_2$ ). Note: signals marked with  $\sim$  are derived from the HMBC analysis only.

**$[\text{Re}(\text{PS}_2)_2(\text{L}3)]$  (3).** The crude product was dissolved in a *n*-hexane/dichloromethane mixture (1:1; 1 mL), loaded onto a  $\text{SiO}_2$  column set for dry column flash chromatography, and eluted with dichloromethane (5 mL  $\times$  3) and dichloromethane/methanol 97:3 (5 mL  $\times$  3). A bright-green band was separated and collected. The eluate was evaporated by a gentle dinitrogen stream to yield the pure compound 3. Yield: 75% (methods A, C, and D); 65% (method B). Elem anal. Calcd for  $\text{C}_{39}\text{H}_{44}\text{NP}_2\text{ReS}_4$  (MW = 903.14): C, 51.86; H, 4.91; N, 1.55. Found: C, 52.02; H, 4.96; N, 1.52. ESI(+)-MS:  $m/z$  709.03 ( $[\text{M} - 194]^+$ , 100%, assignable to the  $[\text{Re}(\text{PS}_2)_2(\text{SH})]^+$  species); 903.14 ( $\text{M}^+$ , 50%).  $^{31}\text{P}$  NMR (161.98 MHz,  $\text{CD}_2\text{Cl}_2$ ):  $\delta$  27.04 (s).  $^1\text{H}$  NMR (400 MHz,  $\text{CD}_2\text{Cl}_2$ ):  $\delta$  1.54, 1.57, 1.64, 1.96 (m, 13H,  $\text{H}_{\text{adamantane}}$ ); 2.46, 2.85 (2 m, 2H + 2H,  $\text{PCH}_2\text{CH}_2\text{S}$ ); 2.97, 3.38 (2 m, 2H + 2H,  $\text{PCH}_2\text{CH}_2\text{S}$ ); 5.50 (1H,  $\text{S}_2\text{CNH}$ ); 7.38 (m, 2H,  $\text{H}_{\text{arom}}$  p'); 7.38 (m, 4H,  $\text{H}_{\text{arom}}$  m'); 7.39 (m, 2H,  $\text{H}_{\text{arom}}$  p); 7.42 (m, 4H,  $\text{H}_{\text{arom}}$  m); 7.52 (m, 4H,  $\text{H}_{\text{arom}}$  o'); 7.71 (m, 4H,  $\text{H}_{\text{arom}}$  o).  $^{13}\text{C}$  NMR (100 MHz,  $\text{CD}_2\text{Cl}_2$ ):  $\delta$  29.59, 35.93, 41.13 (3s,  $\text{C}_{\text{adamantane}}$ ); 36.45 (m,  $\text{PCH}_2\text{CH}_2\text{S}$ ); 54.38 (m,  $\text{PCH}_2\text{CH}_2\text{S}$ ); 54.77 (s,  $\text{C}_{\text{quat. adamantane}}$ ); 127.74 (s,  $\text{C}_{\text{arom}}$  m'); 127.80 (s,  $\text{C}_{\text{arom}}$  m); 128.62 (s,  $\text{C}_{\text{arom}}$  p'); 129.17 (s,  $\text{C}_{\text{arom}}$  p); 132.23 (s,  $\text{C}_{\text{arom}}$  o'); 133.08 (s,  $\text{C}_{\text{arom}}$  o);  $\sim$ 137.76 ( $\text{C}_{\text{quat. arom}}$  P);  $\sim$ 139.43 ( $\text{C}_{\text{quat. arom}}$  P);  $\sim$ 187.90 (s,  $\text{CS}_2$ ). Note: signals marked with  $\sim$  are derived from the HMBC analysis only.

**$[\text{Re}(\text{PS}_2)_2(\text{L}4)]$  (4).** The crude product was purified as described for compound 1. Yield: 68% (methods A, C, and D); 58% (method B). Elem anal. Calcd for  $\text{C}_{40}\text{H}_{43}\text{N}_3\text{OP}_2\text{ReS}_4$  (MW = 944.20): C, 50.88; H, 4.59; N, 2.97. Found: C, 51.02; H, 4.66; N, 2.90. ESI(+)-MS:  $m/z$  944.13 ( $\text{M}^+$ , 100%).  $^{31}\text{P}$  NMR (161.98 MHz,  $\text{CD}_2\text{Cl}_2$ ):  $\delta$  27.04 (s).  $^1\text{H}$  NMR (400 MHz,  $\text{CD}_2\text{Cl}_2$ ):  $\delta$  2.40, 2.90 (2m, 2H + 2H,  $\text{PCH}_2\text{CH}_2\text{S}$ ); 2.62 (m, 4H,  $\text{NCH}_2\text{CH}_2\text{N}$  piperazine); 3.03, 3.59 (2m, 2H + 2H,  $\text{PCH}_2\text{CH}_2\text{S}$ ); 3.47 (m, 4H,  $\text{NCH}_2\text{CH}_2\text{N}$  piperazine); 3.82 (s, 3H,  $\text{OCH}_3$ ); 6.81 (m, 1H,  $\text{H}_{\text{arom}}$  o L4); 6.88 (m, 1H,  $\text{H}_{\text{arom}}$  m L4); 6.95 (m, 1H,  $\text{H}_{\text{arom}}$  m L4); 7.04 (m, 1H,  $\text{H}_{\text{arom}}$  p L4); 7.28 (m, 2H,  $\text{H}_{\text{arom}}$  p' PS2); 7.35 (m, 4H,  $\text{H}_{\text{arom}}$  m' PS2); 7.40 (m, 2H,  $\text{H}_{\text{arom}}$  p PS2); 7.41 (m, 4H,  $\text{H}_{\text{arom}}$  m PS2); 7.62 (m, 4H,  $\text{H}_{\text{arom}}$  o PS2); 7.64 (m, 4H,  $\text{H}_{\text{arom}}$  o' PS2).  $^{13}\text{C}$  NMR (100 MHz,  $\text{CD}_2\text{Cl}_2$ ):  $\delta$  36.21 (m,  $\text{PCH}_2\text{CH}_2\text{S}$ ); 43.99 ( $\text{NCH}_2\text{CH}_2\text{N}$ ); 49.67 ( $\text{NCH}_2\text{CH}_2\text{N}$ ); 55.20 (s,  $\text{PCH}_2\text{CH}_2\text{S}$ ); 55.21 (s,  $\text{OCH}_3$ ); 111.44 (s,  $\text{C}_{\text{arom}}$  m L4); 118.29 (s,  $\text{C}_{\text{arom}}$  o L4); 120.85 (s,  $\text{C}_{\text{arom}}$  m' L4); 123.21 (s,  $\text{C}_{\text{arom}}$  p L4); 127.12 (s,  $\text{C}_{\text{arom}}$  m' PS2); 127.87 (s,  $\text{C}_{\text{arom}}$  m PS2); 128.52 (s,  $\text{C}_{\text{arom}}$  p' PS2); 129.31 (s,  $\text{C}_{\text{arom}}$  p PS2); 132.30 (s,  $\text{C}_{\text{arom}}$  o' PS2); 133.24 (s,  $\text{C}_{\text{arom}}$  o PS2);  $\sim$ 137.35 ( $\text{C}_{\text{quat. arom}}$  P PS2);  $\sim$ 139.15 ( $\text{C}_{\text{quat. arom}}$  P PS2);  $\sim$ 140.70 ( $\text{C}_{\text{quat. arom}}$  N L4);  $\sim$ 152.20 ( $\text{C}_{\text{quat. arom}}$   $\text{OCH}_3$  L4);  $\sim$ 199.22 (s,  $\text{CS}_2$ ).

Note: signals marked with ~ are derived from the HMBC analysis only.

**[Re(PS)<sub>2</sub>(L5)] (5).** The crude product was purified as described for compound 3. Yield: 66% (methods A, C, and D). Elem anal. Calcd for C<sub>42</sub>H<sub>48</sub>N<sub>3</sub>O<sub>2</sub>ReS<sub>4</sub> (MW = 987.26): C, 51.10; H, 4.90; N, 4.26. Found: C, 51.22; H, 4.99; N, 4.18. ESI(+)-MS: *m/z* 493.58 ([M + H]<sup>2+</sup>, 100%); 987.16 (M<sup>+</sup>, 10%). <sup>31</sup>P NMR (161.98 MHz, CD<sub>2</sub>Cl<sub>2</sub>): δ 26.77 (s); 26.99 (s). <sup>1</sup>H NMR (400 MHz, CD<sub>2</sub>Cl<sub>2</sub>): δ 2.21 (m, 2H, NHCH<sub>2</sub>CH<sub>2</sub>N); 2.42, 2.86 (2 m, 2H + 2H, PCH<sub>2</sub>CH<sub>2</sub>S); 2.43 (m, 4H, NCH<sub>2</sub>CH<sub>2</sub>N piperazine); 2.99 (m, 4H, NCH<sub>2</sub>CH<sub>2</sub>N piperazine); 3.03, 3.11 (2 m, 2H + 2H, PCH<sub>2</sub>CH<sub>2</sub>S); 3.08 (m, 2H, NHCH<sub>2</sub>CH<sub>2</sub>N); 3.86 (s, 3H, OCH<sub>3</sub>); 6.22 (m, 1H, NHCH<sub>2</sub>CH<sub>2</sub>N); 6.89 (m, 1H, H<sub>arom</sub> m LS); 6.93 (m, 1H, H<sub>arom</sub> o LS); 6.94 (m, 1H, H<sub>arom</sub> m LS); 7.00 (m, 1H, H<sub>arom</sub> p LS); 7.32 (m, 2H, H<sub>arom</sub> p PS2); 7.38 (m, 4H, H<sub>arom</sub> m PS2); 7.39 (m, 2H, H<sub>arom</sub> p' PS2); 7.39 (m, 4H, H<sub>arom</sub> m' PS2); 7.57 (m, 4H, H<sub>arom</sub> o' PS2); 7.68 (m, 4H, H<sub>arom</sub> o PS2). <sup>13</sup>C NMR (100 MHz, CD<sub>2</sub>Cl<sub>2</sub>): δ 36.32 (m, PCH<sub>2</sub>CH<sub>2</sub>S); 38.38 (s, PCH<sub>2</sub>CH<sub>2</sub>S); 50.24 (s, NCH<sub>2</sub>CH<sub>2</sub>N piperazine); 50.33 (NHCH<sub>2</sub>CH<sub>2</sub>N); 52.77 (s, NCH<sub>2</sub>CH<sub>2</sub>N piperazine); 55.15 (s, OCH<sub>3</sub>); 55.17 (NHCH<sub>2</sub>CH<sub>2</sub>N); 111.46 (s, C<sub>arom</sub> m LS); 118.12 (s, C<sub>arom</sub> o LS); 120.99 (s, C<sub>arom</sub> m' LS); 122.66 (s, C<sub>arom</sub> p LS); 127.27 (s, C<sub>arom</sub> m PS2); 127.84 (s, C<sub>arom</sub> m' PS2); 128.55 (s, C<sub>arom</sub> p PS2); 129.28 (s, C<sub>arom</sub> p' PS2); 132.28 (s, C<sub>arom</sub> o PS2); 133.11 (s, C<sub>arom</sub> o' PS2); ~137.47 (C<sub>quat</sub> arom P); ~139.10 (C<sub>quat</sub> arom P); ~141.50 (C<sub>quat</sub> arom N); ~152.40 (C<sub>quat</sub> arom OCH<sub>3</sub>); ~203.42 (s, CS<sub>2</sub>). Note: signals marked with ~ are derived from the HMBC analysis only.

**[Re(PS)<sub>2</sub>(L6)] (6).** The crude product was purified as described for compound 3. Yield: 68% (methods A, C, and D). Elem anal. Calcd for C<sub>44</sub>H<sub>52</sub>N<sub>3</sub>O<sub>2</sub>ReS<sub>4</sub> (MW = 1014.32): C, 52.05; H, 5.16; N, 4.14. Found: C, 52.12; H, 5.20; N, 4.10. ESI(+)-MS: *m/z* 507.59 ([M + H]<sup>2+</sup>, 100%); 1014.32 (M<sup>+</sup>, 10%). <sup>31</sup>P NMR (161.98 MHz, CD<sub>2</sub>Cl<sub>2</sub>): δ 25.70 (s); 25.76 (s). <sup>1</sup>H NMR (400 MHz, CD<sub>2</sub>Cl<sub>2</sub>): δ 1.31 (m, 2H, NHCH<sub>2</sub>CH<sub>2</sub>CH<sub>2</sub>CH<sub>2</sub>N); 1.42 (m, 2H, NHCH<sub>2</sub>CH<sub>2</sub>CH<sub>2</sub>CH<sub>2</sub>N); 2.17 (m, 2H, NHCH<sub>2</sub>CH<sub>2</sub>CH<sub>2</sub>CH<sub>2</sub>N); 2.41, 2.86 (2m, 2H + 2H, PCH<sub>2</sub>CH<sub>2</sub>S); 2.49 (m, 4H, NCH<sub>2</sub>CH<sub>2</sub>N piperazine); 3.00 (m, 2H, NHCH<sub>2</sub>CH<sub>2</sub>CH<sub>2</sub>CH<sub>2</sub>N); 3.03, 3.53 (2m, 2H + 2H, PCH<sub>2</sub>CH<sub>2</sub>S); 3.04 (m, 4H, NCH<sub>2</sub>CH<sub>2</sub>N piperazine); 3.86 (s, 3H, OCH<sub>3</sub>); 6.89 (m, 1H, H<sub>arom</sub> o L6); 6.91 (m, 1H, H<sub>arom</sub> m L6); 6.94 (m, 1H, H<sub>arom</sub> m L6); 7.01 (m, 1H, H<sub>arom</sub> p L6); 7.32 (m, 6H, H<sub>arom</sub> p + m PS2); 7.37 (m, 6H, H<sub>arom</sub> p' + m' PS2); 7.57 (m, 4H, H<sub>arom</sub> o' PS2); 7.68 (m, 4H, H<sub>arom</sub> o PS2); 8.44 (m, 1H, NHCH<sub>2</sub>CH<sub>2</sub>CH<sub>2</sub>CH<sub>2</sub>N). <sup>13</sup>C NMR (100 MHz, CD<sub>2</sub>Cl<sub>2</sub>): δ 24.44 (s, NHCH<sub>2</sub>CH<sub>2</sub>CH<sub>2</sub>CH<sub>2</sub>N); 26.34 (s, NHCH<sub>2</sub>CH<sub>2</sub>CH<sub>2</sub>CH<sub>2</sub>N); 36.30 (m, PCH<sub>2</sub>CH<sub>2</sub>S); 42.08 (s, NHCH<sub>2</sub>CH<sub>2</sub>CH<sub>2</sub>CH<sub>2</sub>N); 49.92 (NCH<sub>2</sub>CH<sub>2</sub>N piperazine); 52.97 (s, NCH<sub>2</sub>CH<sub>2</sub>N piperazine); 55.22 (s, OCH<sub>3</sub>); 55.38 (s, PCH<sub>2</sub>CH<sub>2</sub>S); 57.18 (NHCH<sub>2</sub>CH<sub>2</sub>CH<sub>2</sub>CH<sub>2</sub>N); 111.36 (s, C<sub>arom</sub> o L6); 118.38 (s, C<sub>arom</sub> m L6); 122.66 (s, C<sub>arom</sub> m' L6); 122.86 (s, C<sub>arom</sub> p L6); 127.25 (s, C<sub>arom</sub> m PS2); 127.81 (s, C<sub>arom</sub> m' PS2); 128.46 (s, C<sub>arom</sub> p PS2); 129.18 (s, C<sub>arom</sub> p' PS2); 132.38 (s, C<sub>arom</sub> o PS2); 133.14 (s, C<sub>arom</sub> o' PS2); ~137.69 (C<sub>quat</sub> arom P); ~139.49 (C<sub>quat</sub> arom P); ~141.40 (C<sub>quat</sub> arom N); ~152.60 (C<sub>quat</sub> arom OCH<sub>3</sub>); 202.28 (s, CS<sub>2</sub>). Note: signals marked with ~ are derived from the HMBC analysis only.

**[Re(PScy)<sub>2</sub>(L1)] (7).** The crude product was purified as described for compound 1. Yield: 74% (methods A, C, and D). Elem anal. Calcd for C<sub>33</sub>H<sub>60</sub>NP<sub>2</sub>ReS<sub>4</sub> (MW = 847.25): C, 46.78; H, 7.14; N, 1.65. Found: C, 46.52; H, 7.03; N, 1.74. ESI(+)-MS: *m/z* 847.25 (M<sup>+</sup>, 100%). <sup>31</sup>P NMR (161.98 MHz, CD<sub>2</sub>Cl<sub>2</sub>): δ 19.07 (s, br Δν<sub>1/2</sub> ≈ 50 Hz). <sup>1</sup>H NMR (400 MHz, CD<sub>2</sub>Cl<sub>2</sub>): δ 1.00–1.65 (series of m, 40H, CH<sub>2</sub> groups of cyclohexyl rings); 1.90, 2.13 (2m, 2H + 2H, PCH<sub>2</sub>CH<sub>2</sub>S); 1.72 (m, 2H, N(CH<sub>2</sub>CH<sub>2</sub>)<sub>2</sub>); 2.43 (m, 2H, PCH'); 2.56 (m, 2H, PCH); 3.25, 3.46 (2 m, 2H + 2H, PCH<sub>2</sub>CH<sub>2</sub>S); 3.64 (m, 4H, N(CH<sub>2</sub>CH<sub>2</sub>)<sub>2</sub>). <sup>13</sup>C NMR (100 MHz, CD<sub>2</sub>Cl<sub>2</sub>): δ 24.97 (s, N(CH<sub>2</sub>CH<sub>2</sub>)<sub>2</sub>); 27.58 (s, PCH(CH<sub>2</sub>CH<sub>2</sub>)<sub>2</sub>CH<sub>2</sub>); 26.95 (s, PCH(CH<sub>2</sub>CH<sub>2</sub>)<sub>2</sub>CH<sub>2</sub>); 28.35 (s, PCH(CH<sub>2</sub>CH<sub>2</sub>)<sub>2</sub>CH<sub>2</sub>); 28.93 (s, PCH(CH<sub>2</sub>CH<sub>2</sub>)<sub>2</sub>CH<sub>2</sub>); 29.65 (s, PCH(CH<sub>2</sub>CH<sub>2</sub>)<sub>2</sub>CH<sub>2</sub>); 29.93 (s, PCH(CH<sub>2</sub>CH<sub>2</sub>)<sub>2</sub>CH<sub>2</sub>); 31.58 (m, PCH<sub>2</sub>CH<sub>2</sub>S); 32.35 (s, PCH(CH<sub>2</sub>CH<sub>2</sub>)<sub>2</sub>CH<sub>2</sub>); 32.48 (s, PCH(CH<sub>2</sub>CH<sub>2</sub>)<sub>2</sub>CH<sub>2</sub>); 32.75 (s, PCH(CH<sub>2</sub>CH<sub>2</sub>)<sub>2</sub>CH<sub>2</sub>); 32.98 (s, PCH(CH<sub>2</sub>CH<sub>2</sub>)<sub>2</sub>CH<sub>2</sub>); 33.61 (m, PCH(CH<sub>2</sub>CH<sub>2</sub>)<sub>2</sub>CH<sub>2</sub>); 33.93 (m, PCH(CH<sub>2</sub>CH<sub>2</sub>)<sub>2</sub>CH<sub>2</sub>); 47.02 (s, N(CH<sub>2</sub>CH<sub>2</sub>)<sub>2</sub>); 60.05 (s, PCH<sub>2</sub>CH<sub>2</sub>S); 199.81 (CS<sub>2</sub>).

**[Re(PSiso)<sub>2</sub>(L1)] (8).** The crude product was purified as described for compound 1. Yield: 74% (methods A, C, and D). Elem anal. Calcd for C<sub>21</sub>H<sub>44</sub>NP<sub>2</sub>ReS<sub>4</sub> (MW = 687.00): C, 36.71; H, 6.46; N, 2.04. Found: C, 36.68; H, 6.51; N, 3.99. ESI(+)-MS: *m/z* 687.14 (M<sup>+</sup>, 100%). <sup>31</sup>P NMR (161.98 MHz, CD<sub>2</sub>Cl<sub>2</sub>): δ 23.77 (s, br Δν<sub>1/2</sub> ≈ 65 Hz). <sup>1</sup>H NMR (400 MHz, CD<sub>2</sub>Cl<sub>2</sub>): δ 1.10 (m, 6H, PCHCH<sub>3</sub>); 1.23 (m, 6H, PCHCH<sub>3</sub>); 1.36 (m, 6H, PCHCH<sub>3</sub>); 1.48 (m, 6H, PCHCH<sub>3</sub>); 1.78 (m, 2H, PCH<sub>2</sub>CH<sub>2</sub>S); 1.96 (m, 2H, N(CH<sub>2</sub>CH<sub>2</sub>)<sub>2</sub>); 1.97 (m, 2H, PCH<sub>2</sub>CH<sub>2</sub>S); 2.69 (m, 2H, PCH'); 2.74 (m, 2H, PCH); 3.05 (m, 2H, SCH<sub>2</sub>CH<sub>2</sub>P); 3.26 (m, 2H, SCH<sub>2</sub>CH<sub>2</sub>P); 3.90 (m, 4H, N(CH<sub>2</sub>CH<sub>2</sub>)<sub>2</sub>). <sup>13</sup>C NMR (100 MHz, CD<sub>2</sub>Cl<sub>2</sub>): δ 18.74 (s, PCHCH<sub>3</sub>); 18.85 (s, PCHCH<sub>3</sub>); 19.28 (s, PCHCH<sub>3</sub>); 20.16 (s, PCHCH<sub>3</sub>); 25.05 (s, N(CH<sub>2</sub>CH<sub>2</sub>)<sub>2</sub>); 28.58 (s, br, PCH'); 30.48 (m, PCH<sub>2</sub>CH<sub>2</sub>S); 30.49 (s, br, PCH); 47.10 (s, N(CH<sub>2</sub>CH<sub>2</sub>)<sub>2</sub>); 59.33 (s, PCH<sub>2</sub>CH<sub>2</sub>S); 197.25 (CS<sub>2</sub>).

**Synthesis of the [<sup>99</sup>Tc(PS)<sub>2</sub>(L)] Complexes (9 and 10).** Method A'. (i) Technetium complexes were prepared following the procedure described for rhenium in method A, starting from [<sup>99</sup>TcCl<sub>3</sub>(MeCN)(PPh<sub>3</sub>)<sub>2</sub>] and using the same stoichiometric ratios.

Method D'. (ii) To an ethanol solution (5 mL) containing [NBu<sub>4</sub>][<sup>99</sup>TcO<sub>4</sub>] (7.9 mg, 0.036 mmol) was added at room temperature under stirring an excess of the selected PSH ligand (0.144 mmol dissolved in 1 mL of ethanol). The solution immediately became red because of the formation of [<sup>99</sup>Tc(PS)<sub>2</sub>(SP=O)].<sup>10</sup> To the mixture was quickly added L1 dissolved in 3 mL of ethanol (0.179 mmol when PS = PS2H and 0.089 mmol when PS = PSisoH). The resulting mixture was stirred at reflux for 30 min. The solvents were removed by a gentle dinitrogen stream, and the crude product was dissolved in the mixture *n*-hexane/dichloromethane (1:1; 1 mL), loaded onto a SiO<sub>2</sub> column set for dry column flash chromatography, and eluted with *n*-hexane/dichloromethane (1:1; 5 mL × 2) and dichloromethane (5 mL × 3) to obtain the pure compounds 9 and 10.

Both <sup>99</sup>Tc complexes were soluble in chlorinated solvents and DMSO, slightly soluble in methanol, *n*-hexane, and diethyl ether, and insoluble in water.

**[<sup>99</sup>Tc(PS)<sub>2</sub>(L1)] (9).** Yield: 77% (method A') and 75% (method D'). Elem anal. Calcd for C<sub>33</sub>H<sub>36</sub>NP<sub>2</sub>S<sub>4</sub><sup>99</sup>Tc (MW = 735.76): C, 53.87; H, 4.93; N, 1.90. Found: C, 53.97; H, 5.03; N, 1.57. ESI(+)-MS: *m/z* 735.36 (M<sup>+</sup>, 100%). <sup>31</sup>P NMR (161.98 MHz, CD<sub>2</sub>Cl<sub>2</sub>): δ 64.28 (s, br, Δν<sub>1/2</sub> ≈ 270 Hz). <sup>1</sup>H NMR (400 MHz, CD<sub>2</sub>Cl<sub>2</sub>): δ 1.63 (m, 4H, N(CH<sub>2</sub>CH<sub>2</sub>)<sub>2</sub>); 2.52 (m, 2H, PCH<sub>2</sub>CH<sub>2</sub>S); 2.96 (m, 2H, N(CH<sub>2</sub>CH<sub>2</sub>)<sub>2</sub>); 3.05 (m, 2H, N(CH<sub>2</sub>CH<sub>2</sub>)<sub>2</sub>); 3.10 (m, 2H, PCH<sub>2</sub>CH<sub>2</sub>S); 3.14 (m, 2H, PCH<sub>2</sub>CH<sub>2</sub>S); 3.94 (m, 2H, PCH<sub>2</sub>CH<sub>2</sub>S); 7.28 (m, 6H, H<sub>arom</sub> p' + m'); 7.36 (m, 6H, H<sub>arom</sub> p + m); 7.53 (m, 4H, H<sub>arom</sub> o); 7.54 (m, 4H, H<sub>arom</sub> o'). <sup>13</sup>C NMR (100 MHz, CD<sub>2</sub>Cl<sub>2</sub>): δ 24.82 (s, N(CH<sub>2</sub>CH<sub>2</sub>)<sub>2</sub>); 32.75 (m, PCH<sub>2</sub>CH<sub>2</sub>S); 45.34 (m, PCH<sub>2</sub>CH<sub>2</sub>S); 48.23 (s, N(CH<sub>2</sub>CH<sub>2</sub>)<sub>2</sub>); 126.83 (s, C<sub>arom</sub> m'); 127.75 (s, C<sub>arom</sub> m); 128.33 (s, C<sub>arom</sub> p'); 129.12 (s, C<sub>arom</sub> p); 132.21 (m, C<sub>arom</sub> o'); 133.06 (m, C<sub>arom</sub> o); ~133.97 (s, C<sub>quat</sub> arom P); ~136.21 (s, C<sub>quat</sub> arom P); 199.35 (CS<sub>2</sub>). Note: signals marked with ~ are derived from the HMBC analysis only.

**[<sup>99</sup>Tc(PSiso)<sub>2</sub>(L1)] (10).** Yield: 67% (method A') and 65% (method D'). Elem anal. Calcd for C<sub>21</sub>H<sub>44</sub>NP<sub>2</sub>S<sub>4</sub><sup>99</sup>Tc (MW 599.69): C, 42.06; H, 7.40; N, 2.34. Found: C, 42.44; H, 7.51; N, 2.23. ESI(+)-MS: *m/z* 599.80 {100%, [<sup>99</sup>Tc(PSiso)<sub>2</sub>(DTC-L1)]<sup>+</sup>}. <sup>31</sup>P NMR (161.98 MHz, CD<sub>2</sub>Cl<sub>2</sub>): δ 69.80 (s, vbr, Δν<sub>1/2</sub> ≈ 700 Hz). <sup>1</sup>H NMR (400 MHz, CD<sub>2</sub>Cl<sub>2</sub>): δ 1.00 (m, 6H, PCHCH<sub>3</sub>); 1.10 (m, 6H, PCHCH<sub>3</sub>); 1.22 (m, 6H, PCHCH<sub>3</sub>); 1.34 (m, 6H, PCHCH<sub>3</sub>); 1.91 (m, 2H, N(CH<sub>2</sub>CH<sub>2</sub>)<sub>2</sub>); 2.0 (m, 2H, PCH<sub>2</sub>CH<sub>2</sub>S); 2.1 (s, br, 2H, PCH), 2.11 (m, 2H, PCH<sub>2</sub>CH<sub>2</sub>S); 2.52 (m, 2H, PCH'); 3.08 (m, 2H, SCH<sub>2</sub>CH<sub>2</sub>P); 3.65 (m, 2H, SCH<sub>2</sub>CH<sub>2</sub>P); 3.83 (m, br, 4H, N(CH<sub>2</sub>CH<sub>2</sub>)<sub>2</sub>). <sup>13</sup>C NMR (100 MHz, CD<sub>2</sub>Cl<sub>2</sub>): δ 18.4 (s, PCHCH<sub>3</sub>); 18.61 (s, PCHCH<sub>3</sub>); 19.3 (s, PCHCH<sub>3</sub>); 19.95 (s, PCHCH<sub>3</sub>); 25.13 (s, N(CH<sub>2</sub>CH<sub>2</sub>)<sub>2</sub>); 25.29 (m, PCH'); 26.00 (m, PCH); 26.10 (m, PCH<sub>2</sub>CH<sub>2</sub>S); 47.9 (s, PCH<sub>2</sub>CH<sub>2</sub>S); 48.0 (s, N(CH<sub>2</sub>CH<sub>2</sub>)<sub>2</sub>); 193.54 (CS<sub>2</sub>).

**X-ray Crystallography.** Single crystals of 1, 2, 7, and 9 suitable for X-ray analysis were grown by the slow diffusion of *n*-hexane into a dichloromethane solution.

**Complexes 1, 2, and 9.** The measurements were collected at room temperature on an Oxford Diffraction/Agilent Gemini E diffractometer using graphite-monochromated Mo K $\alpha$  radiation ( $\lambda = 0.71073 \text{ \AA}$ ). The diffraction intensities were corrected for Lorentz and polarization effects and also for absorption. Empirical multiscan absorption corrections using equivalent reflections were performed with the scaling algorithm *SCALE3 ABSPACK*. Data collection, reduction, and finalization were done with the *CrysAlisPro* software.<sup>16</sup> Accurate unit-cell parameters were determined by least-squares refinement of the 8404 (1), 32995 (2), 19175 (9) strongest reflections chosen from the whole experiment. Two reference frames were collected after every 50 frames in order to investigate crystal deterioration; no sign of systematic changes was noticed either in the peak positions or in the intensities. The structures were solved by means of heavy-atom methods using *SHELXTL-NT*<sup>17</sup> and refined by full-matrix least-squares methods based on  $F_o^2$  with *SHELXL-97*.<sup>18</sup>

**Complex 7.** The measurements were collected at room temperature on a Philips PW1100 diffractometer with graphite-monochromated Mo K $\alpha$  radiation ( $\lambda = 0.71073 \text{ \AA}$ ) and corrected for Lorentz/polarization effects. An absorption correction was also performed by means of  $\Psi$  scans.<sup>16</sup> The unit-cell parameters were determined by least-squares refinement of 30 well-centered high-angle reflections, and three standard reflections were checked every 100 measurements to ensure crystal and equipment stability. No sign of deterioration was detected. The structure was solved by direct methods with *SHELXTL-NT* and refined by standard full-matrix least squares based on  $F_o^2$  with the *SHELXL-97* program.

An extended comment about the refinement of crystallographic structures is given in the Supporting Information

## RESULTS AND DISCUSSION

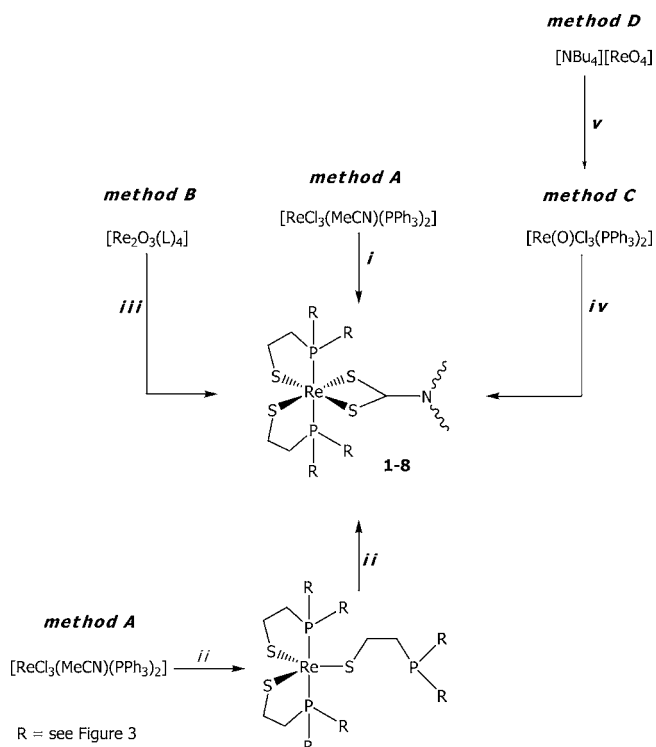
A new class of neutral six-coordinated mixed-ligand M<sup>III</sup> complexes of the general formula  $[M(\text{PS})_2(\text{L})]$  (M = Re, <sup>99</sup>Tc) were easily prepared by ligand-exchange or redox-substitution reactions using precursors in which the metal was in different oxidation states (III, V, and VII), according to the pathways of synthesis sketched in Schemes 1 and 2. Schematic drawings of the obtained  $[M(\text{PS})_2(\text{L})]$  compounds are shown in Figure 3.

Variation of the substituents on the backbone of both phosphinothiolate and dithiocarbamate ligands did not significantly modify the reaction profile or the recovered yields.

In all cases, the reaction progress was followed by TLC: the complexes appeared as bright-green or orange spots for Re or <sup>99</sup>Tc, respectively, with  $R_f$  values in the range 0.6–0.8. TLC analysis carried out on the pure products indicated that (i) isostructural technetium and rhenium complexes showed identical  $R_f$  values; (ii) no significant differences in the  $R_f$  values were observed between compounds bearing diarylphosphinothiolate (**1** and **9**) or trialkylphosphinothiolate (**7**, **8**, and **10**) ligands; (iii) **1** and **4** are the most lipophilic compounds of the series; (iv) modification of the dithiocarbamate backbones yielded a modification of the lipophilic character of the final complex. The introduction of functional or pharmacophore groups such as ester (L2) or (2-methoxyphenyl)piperazine (2-MPP), L4–L6, is responsible for the enhanced hydrophilic character of the complex.

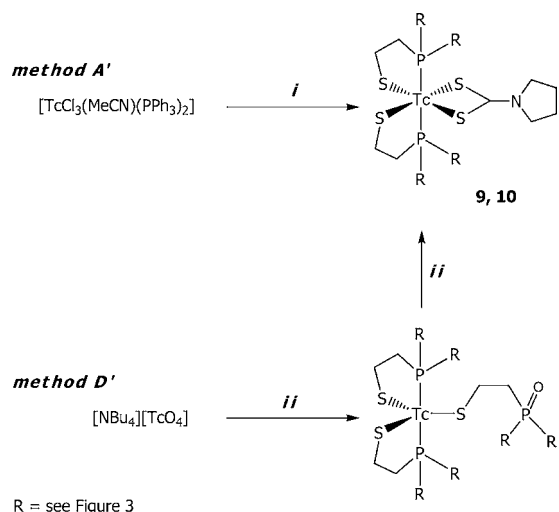
According to methods A and A',  $[M(\text{PS})_2(\text{L})]$  (M = Re, <sup>99</sup>Tc) complexes were easily prepared via ligand-exchange reaction by treating the  $[M\text{Cl}_3(\text{MeCN})(\text{PPh}_3)_2]$  precursor with the selected phosphinothiolate and dithiocarbamate ligands. Similar results were achieved starting from  $[\text{ReCl}_3(\text{MeCN})(\text{PPh}_3)_2]$  by a two-step reaction (method A, pathway ii), which entailed the in situ formation of the  $[\text{Re}(\text{PS})_2(\text{S}^n\text{P})]$  intermediate<sup>11</sup> (detected by ESI(+)-MS:  $[\text{Re}(\text{PS}_2)_2(\text{S-PS}_2)]$ ,

## Scheme 1<sup>a</sup>



<sup>a</sup>Method A: (i) PS (3 equiv), L (5 equiv when PS = PS2 and 2.5 equiv when PS = PSiso or PScy), toluene/EtOH, reflux, 1 h; (ii) (1) PS (3 equiv), toluene/EtOH, reflux, 30 min; (2) L (3 equiv when PS = PS2 and 2.5 equiv when PS = PSiso or PScy). Method B: (iii) PS (6 equiv), toluene/EtOH, reflux, 24 h. Method C: (iv) PS (3.5 equiv), L (5 equiv when PS = PS2 and 2.5 equiv when PS = PSiso or PScy), toluene/EtOH, reflux, 1 h. Method D: (v) excess PPh<sub>3</sub>, excess HCl<sub>concentrated</sub>, MeOH, reflux, 1 h; (iv) PS (3.5 equiv), L (5 equiv when PS = PS2 and 2.5 equiv when PS = PSiso or PScy), MeOH, reflux, 1 h.

## Scheme 2<sup>a</sup>



<sup>a</sup>(i) PS (3 equiv), L1 (5 equiv when PS = PS2 and 2.5 equiv when PS = PSiso), toluene/EtOH, reflux, 1 h; (ii) (1) PS (4 equiv), EtOH, room temperature; (2) L1 (3 equiv when PS = PS2 and 2.5 equiv when PS = PSiso), reflux, 30 min.

$m/z$  922;  $[\text{Re}(\text{PSiso})_2(\text{S-PSiso})]$ ,  $m/z$  599) followed by the addition of L to the reaction mixture.

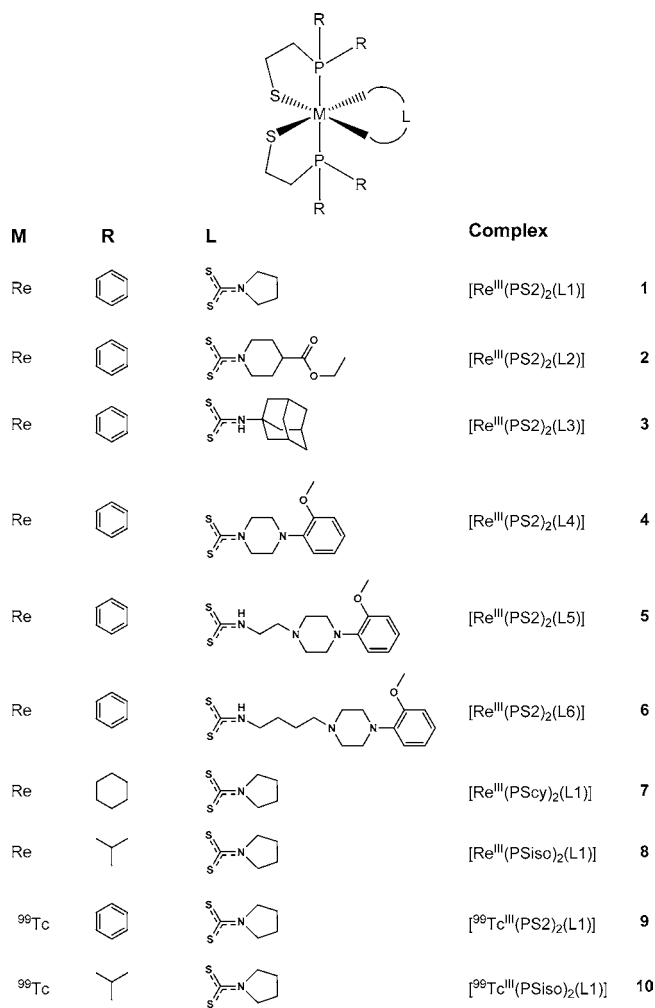


Figure 3. Complexes obtained in our studies.

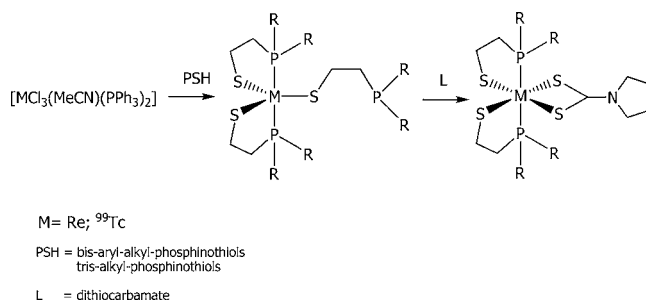
Accurate control of the  $[\text{MCl}_3(\text{MeCN})(\text{PPh}_3)_2]/\text{PS}/\text{L}$  stoichiometric ratios is required to allow collection of the final species in good yield. These ratios were quantified as 1:3:5 and 1:3:2.5 when the phosphinothiolate ligand was PS2H and PS<sub>2</sub>CH or PS<sub>2</sub>SiOH, respectively.

Deviation from these  $[\text{MCl}_3(\text{MeCN})(\text{PPh}_3)_2]/\text{PSH}/\text{L}$  stoichiometric ratios determines a significant reduction of the yield of the final complex. In particular, five-coordinated  $[\text{M}(\text{PS})_2(\text{S}^{\text{R}}\text{P})]$  complexes were observed as byproducts when the reaction was carried out using an insufficient amount of dithiocarbamate to indicate that whereas the formation of the stable  $[\text{M}^{\text{III}}(\text{PS})_2]^+$  moiety was straightforward, the remaining coordinating positions were subject to an exchange equilibrium in which PS and L are in competition. Anyway, the intermediate  $[\text{M}(\text{PS})_2(\text{S}^{\text{R}}\text{P})]$  ( $\text{M} = \text{Re}, {}^{99\text{m}}\text{Tc}$ ) was isolated and characterized by a spectroscopic method. Data were found to be in agreement with those previously reported.<sup>11,19b</sup>

This behavior suggests a possible mechanism of formation of the  $[\text{M}(\text{PS})_2(\text{L})]$  complexes, which requires the initial production of five-coordinated  $[\text{M}(\text{PS})_2(\text{S}^{\text{R}}\text{P})]$  species and subsequent replacement of the monodentate phosphinothiol ligand of  $[\text{M}(\text{PS})_2(\text{S}^{\text{R}}\text{P})]$  with the dithiocarbamate ligand according to Scheme 3.

To confirm the hypothesized mechanism, a reaction was carried out starting from the pure  $[\text{Re}(\text{PS})_2(\text{S}^{\text{R}}\text{P})]$  complex, which was reacted, at reflux, with an excess (3 equiv) of the

Scheme 3



dithiocarbamate ligand (L1). The monodentate phosphinothiol ligand was promptly replaced by the bidentate dithiocarbamate, allowing formation of the six-coordinated  $\text{M}^{\text{III}}$  complex.

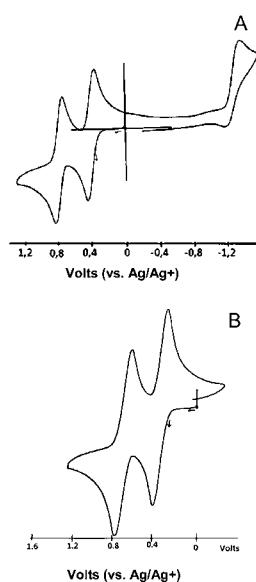
It is worth noting that all attempts to prepare five-coordinated  $[\text{M}(\text{PS})_2(\text{S}^{\text{R}}\text{P})]$  complexes, where  $\text{S}^{\text{R}}$  is a thiol, starting from  $[\text{M}(\text{PS})_2(\text{S}^{\text{R}}\text{P})]$  by substitution of the phosphinothiol with a monodentate aliphatic or aromatic thiol failed,<sup>11</sup> underlining the incapability of thiol to compete with phosphinothiolate in exchange reactions. Hence, only an appropriate selection of the chelating system allowed the preparation of a new series of mixed-ligand complexes containing the  $[\text{M}^{\text{III}}(\text{PS})_2]^+$  moiety.

As outlined in method B,  $[\text{Re}(\text{PS})_2(\text{L})]$  complexes were prepared starting from the dinuclear  $\mu$ -oxorhenium(V) intermediate  $[\text{Re}_2\text{O}_3(\text{L})_4]$  complexes following the procedure reported by Dilworth et al. for synthesis of the  $\{\text{Re}[\text{Ph}_2\text{P}(\text{C}_6\text{H}_4\text{S}-2)]_2(\text{S}_2\text{CNEt}_2)\} \cdot \text{Me}_2\text{CO}$  analogue.<sup>12</sup> This way of synthesis was explored for four selected complexes (1-4). Thus,  $[\text{Re}_2\text{O}_3(\text{L})_4]$  ( $\text{L} = \text{L1-L4}$ ) intermediate complexes were prepared, characterized (Supporting Information), and set to react with phosphinothiol. In these redox-substitution reactions, PSH acted as both a reducing and a coordinating agent, giving the final neutral six-coordinated  $\text{Re}^{\text{III}}$  complexes in moderate yield. Attempts to improve the reaction yield by increasing the amount of phosphinothiol ligand and the reaction time or changing the reaction solvents failed. This behavior is probably due to the overall low solubility of the  $\mu$ -oxo intermediate complexes in the reaction solvents.

Identical  $[\text{Re}(\text{PS})_2(\text{L})]$  complexes were prepared by reacting the  $[\text{ReOCl}_3(\text{PPh}_3)_2]$  precursor with the selected phosphinothiolate and dithiocarbamate ligands, as sketched in method C, and using a  $[\text{ReOCl}_3(\text{PPh}_3)_2]/\text{PS}/\text{L}$  stoichiometric ratio of 1:3.5:5. In this reduction-ligand exchange reaction, PSH acted as both a reducing and a coordinating agent; thus, further excess of the PSH ligand (3.5 equiv) was required to guarantee formation of the final neutral six-coordinated complex in good yield.

In analogy to <sup>99m</sup>Tc, the currently applied <sup>188/186</sup>Re-labeling methods use  $\text{Na}^{188/186}\text{ReO}_4$  as the starting material. Nevertheless, compared to technetium, rhenium required harsher reaction conditions to be reduced from its original oxidation state, VII, to lower oxidation states, typically V/III. Thus, in radiopharmaceutical preparations, normally milligram amounts of tin chloride or other reducing agents are required for the complete reduction of  $\text{Na}^{188/186}\text{ReO}_4$ . Moreover, complex formation occurs in limited volumes, at high temperature, and under strongly acidic conditions.<sup>1</sup>

Hence, in order to mimic the radiopharmaceutical preparation, use of the permetalate anions in the form of  $[\text{NBu}_4][\text{MO}_4]$  was considered.



	$E_{M(III)/M(II)}$	$E_{M(III)/M(IV)}$	$E_{M(IV)/M(V)}$
[Re(PS2) <sub>2</sub> (L1)]	1	-0,31	0,05
[Re(PS2) <sub>2</sub> (L2)]	2	-0,29	0,09a
[Re(PS2) <sub>2</sub> (L3)]	3	-0,32	0,03
[Re(PS2) <sub>2</sub> (L4)]	4	-0,24	0,12
[Re(PS2) <sub>2</sub> (L5)]	5	-0,38	b
[Re(PS2) <sub>2</sub> (L6)]	6	-0,39	c
[Re(PScy) <sub>2</sub> (L1)]	7	-0,49	0,1
[Re(PSiso) <sub>2</sub> (L1)]	8	-0,51	0,08
[ <sup>99</sup> Tc(PS2) <sub>2</sub> (L1)]	9	-1.88	0,11
[ <sup>99</sup> Tc(PSiso) <sub>2</sub> (L1)]	10	-0,41	0,2

**Figure 4.** Cyclic voltammograms of complexes 9 (A) and 1 (B) and voltammetric data for all of the complexes internally referred to the Fc/Fc<sup>+</sup> couple. Data recorded at 200 mV s<sup>-1</sup>, in dry and degassed dichloromethane with a 0.1 M TBAP supporting electrolyte, a platinum-disk working electrode, and a silver-wire quasi-reference electrode.

Starting from [NBu<sub>4</sub>][ReO<sub>4</sub>], a multistep reaction (Scheme 1; method D) was performed. The first step required the preliminary reduction of perrhenate(VII) to the rhenium(V) species, [ReOCl<sub>3</sub>(PPh<sub>3</sub>)<sub>2</sub>], by using an excess of triphenylphosphine, as the reductant, in a strong acidic media (v). In the second step (iv), the [Re(PS)<sub>2</sub>(L)] complex was obtained in good yield through a ligand-exchange reaction that entails, after neutralization with triethylamine (pH 7.3), the coincident addition of the selected bidentate ligands in [ReO<sub>4</sub>]<sup>-</sup>PSH/L stoichiometric ratios of 1:3.5:5 and 1:3.5:2.5 when the phosphinothiol ligand was PS2H and PScyH or PSisoH, respectively. Despite the recognized redox properties of these PSH ligands,<sup>19</sup> attempts to obtain the same complexes starting from [NBu<sub>4</sub>][ReO<sub>4</sub>] directly using PSH as reducing and coordinating agents gave very low yield.<sup>11</sup> Thus, the use of PPh<sub>3</sub>, as additional reducing agent, was necessary to enhance the reaction yield.

On the contrary, using [NBu<sub>4</sub>][<sup>99</sup>TcO<sub>4</sub>], mixed-ligand complexes were generated in good yield by a redox/substitution reaction using PSH itself as reducing and coordinating agents, at autogenous pH (Scheme 2, method D'). The reaction involved the rapid in situ generation of the [<sup>99</sup>Tc(PS)<sub>2</sub>(SP=O)]<sup>10</sup> intermediate, which promptly underwent substitution of the monodentate thiolate SP=O by the dithiocarbamate chelate to give the final [<sup>99</sup>Tc(PS)<sub>2</sub>(L)] complex. In this case, the [<sup>99</sup>TcO<sub>4</sub>]<sup>-</sup>/PSH/L ratios were 1:4:5 and 1:4:2.5 when phosphinothiol was PS2H or PSisoH, respectively.

The possibility to easily prepare these [M<sup>III</sup>(PS)<sub>2</sub>(L)] complexes, starting from the corresponding permethylate anions, in mild reaction conditions and in high yield, laid a first indication on the feasibility of transferring the synthesis at the tracer level for the preparation of <sup>99m</sup>Tc/<sup>188</sup>Re compounds.

**Characterization.** The isolated complexes were fully characterized by elemental analysis, ESI(+)-MS, multinuclear NMR spectroscopy, and cyclic voltammetry. X-ray diffraction analysis was performed on suitable single crystals of compounds 1, 2, 7, and 9.

Physical and chemical characterization of mixed-substituted compounds indicated that all of them contain the [M<sup>III</sup>(PS)<sub>2</sub>]<sup>+</sup> moiety. In detail, elemental analyses of the pure products were in agreement with the proposed formulations, indicating the absence of crystallization solvents. ESI(+)-MS spectra of the mixed-ligand compounds show the monocationic [M-(PS)<sub>2</sub>(L)]<sup>+</sup>(M<sup>+</sup>) species as the common feature, originating by the extraction of one electron. Reasonably, the nozzle potential set to 90 V could be responsible for the one-electron oxidation of M<sup>III</sup> to M<sup>IV</sup> without changes in the metal coordination sphere.

Mass spectra of 5 and 6 display the presence of two molecular ion peaks at *m/z* 493.58 and 987.16 for 5 and at *m/z* 507.59 and 1014.32 for 6, corresponding to the bicationic, monoprotonated species [M + H]<sup>2+</sup> (main peak) and to the M<sup>+</sup> ion, respectively. For these compounds, the generation of [M + H]<sup>2+</sup> species is attributable to the presence on the dithiocarbamate backbone of a protonable tertiary alkylamino group. With the exception of 3, no evidence of the fragmentation process was detected. For compound 3, the mass spectrum exhibits the presence of two peaks (Figure S1, Supporting Information): one at *m/z* 903 (52% relative abundance) corresponding to the M<sup>+</sup> species generated from the oxidation process and the other at *m/z* 709 (100% relative abundance) corresponding to the [M - 194]<sup>+</sup> fragment. This daughter peak was assigned to the [Re(PS)<sub>2</sub>(SH)]<sup>+</sup> species, resulting from the electron extraction along with the loss of an adamantyl isothiocyanate. This type of fragmentation is in accordance with one of the possible dithiocarbamate decomposition processes,<sup>20</sup> which involved the reaction sketched in Figure S1 in the Supporting Information.

<sup>31</sup>P, <sup>1</sup>H, and <sup>13</sup>C NMR spectra were collected at 298 K in dichloromethane-*d*<sub>2</sub>, and 2D experiments (COSY, TOCSY, HMQC, HMBC, and NOESY) were performed for the complete assignment of the proton and carbon signals. The spectra of all of the complexes show sharp peaks in a narrow window typical of diamagnetic species, in agreement with a



Table 1. Crystallographic Data for Complexes 1, 2, 7, and 9

	1	2	7	9
empirical formula	C <sub>33</sub> H <sub>36</sub> NP <sub>2</sub> S <sub>4</sub> Re	C <sub>37</sub> H <sub>42</sub> NO <sub>2</sub> P <sub>2</sub> S <sub>4</sub> Re	C <sub>33</sub> H <sub>60</sub> NP <sub>2</sub> S <sub>4</sub> Re	C <sub>33</sub> H <sub>36</sub> NP <sub>2</sub> S <sub>4</sub> <sup>99</sup> Tc
fw	823.01	909.10	847.20	734.81
wavelength (Å)/temp (K)	0.71073/296	0.71073/296	0.71073/298	0.71073/298
cryst syst	triclinic	monoclinic	triclinic	triclinic
cryst size (mm <sup>3</sup> )	0.15 × 0.08 × 0.05	0.25 × 0.20 × 0.12	0.20 × 0.15 × 0.10	0.30 × 0.20 × 0.08
space group	P $\bar{1}$ (No. 2)	P 2 <sub>1</sub> /c (No. 14)	P $\bar{1}$ (No. 2)	P $\bar{1}$ (No. 2)
a (Å)	9.934(2)	10.616(2)	9.993(2)	9.9059(4)
b (Å)	11.222(2)	18.990(4)	10.779(3)	11.2652(5)
c (Å)	15.385(3)	19.750(4)	17.715(3)	15.4555(5)
$\alpha$ (deg)	74.41(3)		97.09(3)	74.017(3)
$\beta$ (deg)	85.81(3)	105.18(3)	98.05(2)	85.992(3)
$\gamma$ (deg)	86.61(3)		97.68(2)	86.651(3)
volume (Å <sup>3</sup> )	1646.1(6)	3842.7(13)	1852.7(7)	1652.60(11)
Z (molecules/unit cell)	2	4	2	2
calcd density (Mg m <sup>-3</sup> )	1.660	1.571	1.519	1.477
abs coeff $\mu$ (mm <sup>-1</sup> )	4.066	3.496	3.615	0.810
F(000)	820	1824	868	756
indep (unique) reflns/R <sub>int</sub>	7538/0.028	9479/0.029	6816/0.016	13501/0.063
obsd reflns [ $I > 2\sigma(I)$ ]	6062	7456	6724	8707
data/param/restraints	7538/370/0	9479/462/486	6816/370/0	13481/370/0
GOF <sup>a</sup> on F <sup>2</sup>	0.884	1.003	1.250	0.968
final R indices [ $I > 2\sigma(I)$ ]	R1 <sup>b</sup> = 0.0261, wR2 <sup>c</sup> = 0.0463	R1 <sup>b</sup> = 0.0213, wR2 <sup>c</sup> = 0.0440	R1 <sup>b</sup> = 0.0299, wR2 <sup>c</sup> = 0.0777	R1 <sup>b</sup> = 0.0468, wR2 <sup>c</sup> = 0.0985
largest difference peak and hole (e Å <sup>-3</sup> )	0.849 and -1.430	0.580 and -0.535	1.035 and -0.572	0.951 and -0.693

<sup>a</sup>GOF =  $[\sum(w(F_o^2 - F_c^2)^2)/(N_{obs} - N_{param})]^{1/2}$ , based on all data. <sup>b</sup>R1 =  $\sum(|F_o| - |F_c|)/\sum|F_o|$ . <sup>c</sup>wR2 =  $\{\sum[w(F_o^2 - F_c^2)^2]/\sum[w(F_o^2)^2]\}^{1/2}$ .

low-spin d<sup>4</sup> electron configuration typical of trigonal-prismatic M<sup>III</sup> compounds (vide infra).

In general, <sup>31</sup>P NMR spectra show a singlet typical of two magnetic equivalent phosphorus atoms in the range of  $\delta$  19.07–27.04 for the rhenium complexes and at  $\delta$  64.28 and  $\delta$  69.75 for <sup>99</sup>Tc derivatives **9** and **10**, respectively. The signals are significantly downfield-shifted compared with the corresponding ones of uncoordinated phosphinothiol ligands ( $\delta$  -20.0, 5.1, and 3.6 for PS<sub>2</sub>H, PScyH, and PSisoH, respectively). As was previously observed for other phosphinothiolate M<sup>III</sup>/M<sup>V</sup>≡N (M = <sup>99</sup>Tc, Re) complexes,<sup>19d</sup> the magnitude of the coordination chemical shift ( $\Delta$ ) value for phosphinothiolate phosphorus atom is a function of the phosphine Tolman cone angle: small cone angles determine larger shifts, whereas larger cone angles determine smaller shifts.<sup>21</sup>

In <sup>99</sup>Tc complexes (**9** and **10**), the <sup>31</sup>P signals appear notably broadened and downfield-shifted compared to the corresponding signal in the rhenium analogues (**9**,  $\Delta\nu_{1/2}$  ca. 270 Hz; **10**,  $\Delta\nu_{1/2}$  ca. 700). This behavior has already been attributed to the coupling of the <sup>31</sup>P nuclear spin with the quadrupole of the <sup>99</sup>Tc nucleus.<sup>22,19b</sup> A splitting of the <sup>31</sup>P signal in two different peaks was observed in complexes **5** and **6** (**5**,  $\delta$  26.77 and 26.99 ppm; **6**,  $\delta$  25.70 and 25.76 ppm) to indicate the presence of two magnetically nonequivalent phosphorus atoms probably because of conformational changes of the molecule.

Both <sup>1</sup>H and <sup>13</sup>C NMR spectra, of each compound, are very informative and clearly display sets of signals corresponding to the phosphinothiolate and dithiocarbamate ligands. As an example, the 1D and 2D <sup>1</sup>H,<sup>1</sup>H COSY,<sup>1</sup>H-<sup>1</sup>H NOESY, <sup>1</sup>H-<sup>13</sup>C HMQC, and <sup>1</sup>H-<sup>13</sup>C HMBC maps of complex **9** are sketched in Figure S2 (Supporting Information), together with the <sup>1</sup>H-<sup>31</sup>P HMBC map, displaying scalar interactions of the <sup>31</sup>P nucleus and the phenyl and side chain CH<sub>2</sub>CH<sub>2</sub> protons.

All of the complexes were found to be stable in air and in dichloromethane solution. Cyclic voltammetry was performed on all of the complexes to explore their redox properties. Data are reported in Figure 4 along with cyclic voltammograms of selected rhenium and <sup>99</sup>Tc [M(PS)<sub>2</sub>(L)] analogues (**1** and **9**) as representative examples.

In general, two reversible one-electron oxidations were observed for all complexes. It is worth noting that a further reversible one-electron reduction was evidenced only for **9**. The oxidations were assigned by coulombometric experiments to the formation of M<sup>IV</sup> and M<sup>V</sup> species, respectively, presumably accessing the M<sup>IV</sup> nd<sup>3</sup> ( $n = 4$  and  $5$ ) and M<sup>V</sup> nd<sup>2</sup> ( $n = 4$  and  $5$ ) systems. The reduction was assigned to the Tc<sup>II</sup>/Tc<sup>III</sup> couple.

As expected on the basis of previous investigations on isostructural technetium and rhenium systems, rhenium complexes are generally easier to oxidize and more difficult to reduce with respect to the corresponding technetium compounds. For **8** and **10**, the redox potential gap is at the long end of the range usually observed in pairs of technetium and rhenium homologues.

In detail, considering the pairs of rhenium and technetium [M(PS)<sub>2</sub>(L)] homologues (**1/9** and **8/10**): complexes **1** and **9** were equally stable to the oxidation process, showing in the anodic region almost superimposable cyclic voltammograms, while a reversible Tc<sup>III</sup>/Tc<sup>II</sup> process was evidenced only for **9** at more negative value (-1.88 V). In view of the [M-(PSiso)<sub>2</sub>(L1)] pair (**8** and **10**), the redox potential of **8** indicated that it is easier to oxidize by 100 mV than the corresponding <sup>99</sup>Tc complex (**10**). This latter compound is easier to oxidize by 100 mV with respect to the [<sup>99</sup>Tc-(PS)<sub>2</sub>(L1)] analogue (**9**, where PS<sub>2</sub> is diarylphosphinothiolate). Furthermore, looking inside the rhenium complex series, **1** is more stable than **7** and **8** by 180 and 200 mV, respectively, while compounds **7** and **8**, in which phosphinothiolate was

PScy and PSiso, respectively, have approximately the same potential. Finally, for complex **2**, the Re<sup>IV</sup>/Re<sup>V</sup> oxidation was irreversible (even at 500 mV s<sup>-1</sup> scan speed), while for complexes **5** and **6**, the process was followed by a chemical transformation, whose product oxidized at about 0.40 V (referred to the Fc/Fc<sup>+</sup> couple).

Cyclic voltammetric data show that the redox potential of the compounds was sensitive to changes of the ligand substituents and dependent on the nature of the phosphinothiol ligand. Thus, complexes with trialkylphosphinothiolates are more easily oxidized, by ca. 0.20 V for rhenium compounds and 0.08 V for <sup>99</sup>Tc compounds, than the corresponding bis-(aryllalkyl)phosphinothiolate complexes. These trends could be interpreted in terms of  $\pi$ -back-bonding interaction of d electrons of the M<sup>III</sup> center with appropriate orbitals of the phosphorus atoms, which is expressed as the ability of the ligand to donate or accept charge from the metal center.

It is well-known that phosphines are  $\pi$ -acceptor ligands; this property is stronger for arylphosphine than for alkylphosphine, which, in turn, are considered better  $\sigma$ -donor atoms. Accordingly, the bis(aryllalkyl)phosphinothiol ligand, PS2H, exhibits stronger  $\pi$ -acid character in the series, whereas the trialkylphosphinothiol ligands, PScyH and PSisoH, are better  $\sigma$ -donor and less  $\pi$ -acceptor ligands. Consequently, the strong  $\sigma$ -donor property of PScyH and PSisoH contributed to efficiently stabilize the electron-poor M<sup>IV</sup> species. Actually, when PS2H was replaced by PScyH and PSisoH, the potential for the couple M<sup>III</sup>/M<sup>IV</sup> shifts to a more negative value (see above), indicating that [M(PScy/PSiso)<sub>2</sub>(L)] is more easily oxidized than [M(PS2)<sub>2</sub>(L)]. This fact explains the reason for which control of the workup conditions was required for **8** and **10**. On the other hand, the greater  $\pi$ -acid character of PS2H allow stabilization of the electron-rich M<sup>III</sup> species. This behavior is particularly evident in complex **9**, which is the only one that shows a reduction process to the <sup>99</sup>Tc<sup>II</sup> state: in agreement with the higher stabilizing effect of phosphinothiol, which allows reduction of the complex, and with the greater stability of technetium at low oxidation states compared to rhenium.

With regard to dithiocarbamate, the insertion of electron-withdrawing substituents into the ligand backbone, such as in L2 and L4, which helps to drain the excess of electron density of the metal center, makes the resulting compounds (**2** and **4**) more difficult to oxidize than the corresponding unsubstituted derivatives. On the contrary, the use of electron-donating substituents, as well as the insertion of a group spacer between the dithiocarbamic unit and 2-MPP, which contributes to an increase in the electron density at the metal center, makes the resulting complexes (**3**, **5**, and **6**) easier to oxidize. For such compounds, a shift of  $E_{M^{III}/M^{IV}}$  to a more negative value was observed (Figure 4).

**X-ray Crystallography.** Crystals suitable for X-ray studies of complexes **1**, **2**, **7**, and **9** were obtained by the slow diffusion of *n*-hexane into a saturated dichloromethane solution. Data collection parameters and crystal data are reported in Table 1. Selected bond lengths and angles are listed in Table 2.

The molecular structures of complexes **1**, **2**, **7**, and **9** are depicted as ORTEP<sup>23</sup> diagrams in Figures 5 and 6.

All compounds show a “butterfly” shape because of the phosphinothiolate (PS2) ligands occupying four of the six coordination positions around the metal atom. The “inner core” of complexes **1–9** adopts a distorted trigonal-prismatic environment: this geometry was confirmed by comparing the molecular structures of complexes **1–9** with that of [Re-

**Table 2.** Selected Bond Lengths (Å) and Angles (deg); M = Re, <sup>99</sup>Tc

	1	2	7	9
M–S1	2.5459(10)	2.5181(8)	2.5198(13)	2.5246(6)
M–S2	2.5243(11)	2.5067(7)	2.5203(13)	2.5477(7)
M–S3	2.2510(10)	2.2591(9)	2.2587(13)	2.2652(6)
M–S4	2.2659(11)	2.2619(7)	2.2556(13)	2.2429(6)
M–P1	2.3629(10)	2.3502(7)	2.3804(13)	2.3734(6)
M–P2	2.3676(10)	2.3488(7)	2.3869(13)	2.3711(6)
S3–C4	1.835(3)	1.849(3)	1.848(5)	1.847(3)
S4–C2	1.848(3)	1.849(2)	1.858(5)	1.834(3)
P1–C1	1.829(3)	1.843(2)	1.846(5)	1.843(3)
P2–C3	1.841(3)	1.844(2)	1.850(5)	1.840(2)
P–C <sub>phenyl</sub> <sup>a</sup>	1.839	1.832	1.862	1.838
S1–M–S2	68.29(4)	68.03(3)	68.11(4)	68.34(2)
S1–M–S3	157.19(3)	154.18(2)	156.52(5)	160.05(2)
S2–M–S4	160.60(3)	156.34(2)	152.42(4)	156.59(2)
S3–M–S4	110.47(4)	117.10(3)	118.77(5)	111.63(3)
S3–M–P2	85.86(4)	84.46(3)	85.23(5)	85.67(2)
S4–M–P1	85.58(4)	85.12(2)	84.36(5)	86.03(2)
P1–M–P2	172.50(3)	178.25(2)	170.89(4)	172.67(2)
M–S3–C4	109.64(11)	109.89(8)	111.15(16)	108.78(8)
M–S4–C2	109.02(11)	109.71(8)	111.31(17)	109.71(9)
M–P1–C1	104.31(12)	105.24(8)	105.66(17)	105.69(8)
M–P2–C3	105.91(11)	105.18(8)	104.89(16)	104.00(9)
M–P1–C <sub>phenyl</sub> <sup>b</sup>	120.02	119.56	119.85	119.72
M–P2–C <sub>phenyl</sub> <sup>b</sup>	119.58	120.08	117.39	120.28

<sup>a</sup>Mean of four values. <sup>b</sup>Mean of two values.

(S<sub>3</sub>CPh)<sub>2</sub>(S<sub>2</sub>CPh)],<sup>7a</sup> taken as a reference, using the software MERCURY.<sup>24</sup> It shows that the “inner cores” (including the metal) are essentially superimposable (root-mean-square value within 0.14–0.19 Å).

As expected, **1** and **9** are isostructural and isomorphous (Figure 5).

In all of the complexes, the coordination sphere is characterized by the presence of the relatively uncommon P<sub>2</sub>S<sub>4</sub> coordination environment, where the two  $\pi$ -acceptor phosphorus atoms are in a reciprocal trans position, whereas the sulfur atoms of the phosphinothiolate donors and of the dithiocarbamate ligand are in a reciprocal cis configuration.

A close inspection of the CCDC<sup>12,25–28</sup> database reveals that the compounds described here are the first reported mononuclear six-coordinated M (<sup>99</sup>Tc, Re) complexes showing the P<sub>2</sub>S<sub>4</sub> environment substantiated by a PS moiety with a P–S aliphatic linker.

Upon chelation, the two phosphinothiolate and one dithiocarbamate ligands define two five-membered and one four-membered rings around the metal center, respectively; the five-membered ring, including P1 (or P2), has been designated here as the P1 (or P2) ring. The four-membered ring defined by the M, S1, S2, and C5 atoms is planar in all of the complexes. In **1–9**, the P1 and P2 rings assume an *envelope* (C<sub>s</sub>) arrangement. The departure of the “flap” atoms (C1 or C3, except for P1 in **7**) range from 0.56 to 0.67 Å; the *envelope* arrangement in the P1 ring of **7** is rather twisted and approaches the *half-chair* (C<sub>2</sub>) shape. The calculated mean planes encompassing the five atoms of the P1 and P2 rings of all complexes are roughly orthogonal to the equatorial plane (pertinent dihedral angles ranging from 77.7° to 84.7°) and are

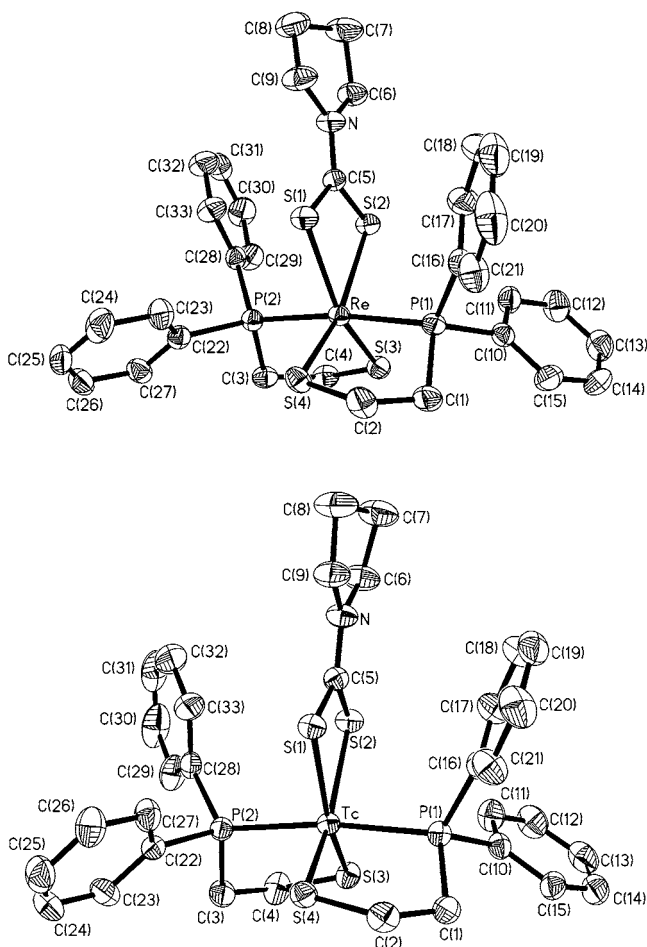


**Figure 5.** ORTEP views of complexes **1** (top) and **9** (bottom), showing the numbering scheme used. Hydrogen atoms have been omitted for clarity, while thermal ellipsoids have been drawn at the 40% probability level.

also roughly orthogonal to each other, making dihedral angles of 72.8°, 58.9°, 52.0°, and 72.3° in the four complexes.

With respect to distances in the coordination sphere (Table 2), the parameters of **1** and **9** look alike, as expected for an isostructural <sup>99</sup>Tc/Re pair. A closest similarity is found in the M–S<sub>L</sub> and M–S<sub>PS</sub> bond lengths. M–P bonds appear only slightly elongated in **1** (difference for the mean value is 0.016 Å). Likewise, the angles involving atoms trans to each other are almost identical: the mean value for S–M–S angles is 158.9° in **1** and 158.3° in **9**, while the P–M–P angle is 172.50(3)° in **1** and 172.67(2)° in **9**.

By a comparison of all of the four compounds **1–9**, it emerges that for each bond type (M–P, M–S<sub>PS</sub>, and M–S<sub>L</sub>) there is always a longer and a shorter distance. In particular, a shorter M–S<sub>PS</sub> distance is always trans to a longer M–S<sub>L</sub> bond and vice versa, so that the sum of the trans M–S distances is the same within 0.004 Å in all complexes. The M–S<sub>PS</sub> lengths do not differ too much in the series (mean values are 2.258, 2.260, 2.257, and 2.254 Å for **1**, **2**, **7**, and **9**, respectively), while the M–S<sub>L</sub> lengths are longer, on average, by about 0.020 Å in **1** and **9** (mean values 2.535 and 2.536 Å) than in **2** and **7** (mean values 2.512 and 2.520 Å). A similar, but reversed trend is seen for M–P distances, which are longer, on average, by the same amount in **2** and **7** (mean values 2.384 and 2.372 Å) than in **1** and **9** (mean values 2.365 and 2.350 Å).

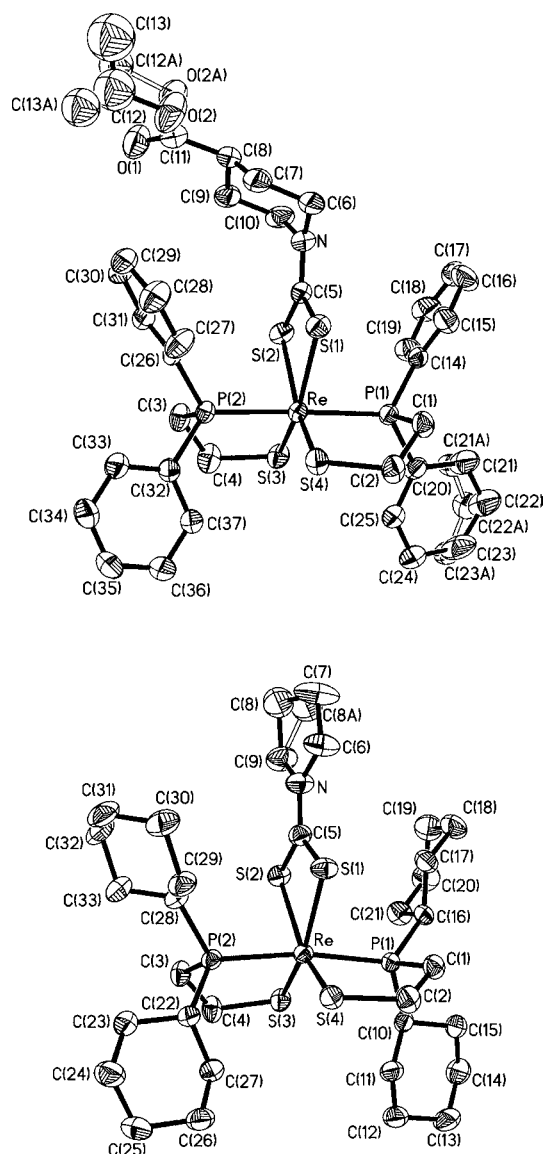


**Figure 6.** ORTEP views of complexes **2** (top) and **7** (bottom), showing the numbering scheme used. Hydrogen atoms have always been omitted for clarity, while thermal ellipsoids have been drawn at the 40% probability level. The alternate positions of the disordered moieties in complexes **2** and **7** have been drawn with white bonds.

The M–P, M–S<sub>PS</sub>, and M–S<sub>L</sub> bond types in the coordination sphere vary in the ranges 2.349(1)–2.387(1), 2.243(1)–2.266(1), and 2.507(1)–2.548(1), respectively. Thus, the two phosphinothiolates look strongly bound to the metal center, while the bond distances between the metal and dithiocarbamate are considerably longer. Also interesting, the C–S and C–N bond lengths of the dithiocarbamate ligand are almost unchanged (ca. 1.700 and 1.330 Å, respectively) in all complexes, pointing to a significant double-bonding character for C–N (and single-bonding character for C–S).

In rhenium complexes, analysis of the M–P distances of **1** and **7** shows an elongation of the M–P bond distance for **7** in accordance with the more marked  $\sigma$ -donor property of PScyH with respect to PS2. Meanwhile, by looking at the Re–S<sub>L</sub> distances, it appears that the Re–S<sub>L</sub> bonds lengthen with increasing of electron-donating character of the ligand donor set on going from **7** to **1** and to **2**. This behavior indicates that

the metal, while accepting more negative charge from the ligand set, needs to redistribute this electron density excess over a larger volume and to transfer electrons more readily in the oxidation processes. In fact, **7** undergoes oxidation to  $\text{Re}^{\text{IV}}$  at a more negative value ( $-0.49$  V) than **1** ( $-0.31$  V) and **2** ( $-0.29$  V).

Thus, for these four compounds, the stoichiometries of the ligands and bond distances within the coordination sphere are in agreement with those observed in the previously reported compounds.<sup>7–9,12</sup> Accordingly, the two identical phosphinothiolate ligands appear to be tightly bound to the metal center, defining the substitution-inert  $[\text{M}^{\text{III}}(\text{PS})_2]^+$  moiety, in which the particular arrangement of the coordinating atoms induces an elongation of the bond distances between the metal and donor atoms of the dithiocarbamate ligand. However, this sort of labilizing effect is counteracted by coordination of the dithiocarbamate itself, which upon coordination produces a neutral species and makes extensive  $\pi$  delocalization through the four-membered S–C–S–M ring possible, as confirmed by the equivalence of the involved M–S bond distance (Table 2).

This structural feature strongly supports the proposed model in which two identical ligands provide two apical transpositioned  $\pi$ -acceptor atoms, connected with two strong cis-positioned  $\sigma$ -donor atoms, whereas the third (chemically different) ligand, characterized by an electronic conjugation within the two donor atoms, binds the metal with quite long bond distances.

## CONCLUSION

This paper represents a further step of our continuous efforts to explore the coordination chemistry of the group 7 metals technetium and rhenium with phosphinothiol and dithiocarbamate ligands.

A series of neutral, lipophilic  $\text{Re}^{\text{III}}$  and  $\text{Tc}^{\text{III}}$  mixed-ligand complexes comprising bis(arylalkyl)- and trialkylphosphinothiolate and dithiocarbamate ligands have been prepared and fully characterized. The formation of these complexes is favored by the chemical properties of the  $[\text{M}^{\text{III}}(\text{PS})_2]^+$  moiety, in which the particular arrangement of atoms around the metal center permits, when reacted with the selected dithiocarbamate ligands, the formation of the final  $[\text{M}(\text{PS})_2(\text{L})]$  complex, in high yield, invariably from the adopted pathway of synthesis. Furthermore, in  $[\text{M}(\text{PS})_2(\text{L})]$  compounds, variation of the substituents on the backbone of the two bidentate ligands (PSH and L) did not alter the stoichiometry, the stereochemistry, and the stability of the resulting compounds but their lipophilicity and redox properties.

This behavior indicates that  $[\text{M}^{\text{III}}(\text{PS})_2]^+$  can be considered as a substitution-inert building block useful for the preparation of new classes of mixed-ligand  $^{99\text{m}}\text{Tc}/^{188}\text{Re}$  compounds. A key advantage of these reactions was that all of the complexes were efficiently prepared by simply mixing both the PSH and L ligands with the metal starting precursors and that in these preparations no detectable formation of the corresponding trisubstituted complexes, comprising identical bidentate ligands, in a trigonal-bipyramidal or in an octahedral environment, was observed. This fact suggests that the  $\text{M}^{\text{III}}\text{P}_2\text{S}_4$  arrangement is the most stable combination of atoms. Clearly, the high stability and kinetic inertness generated by the balance between the  $\text{M}^{\text{III}}$  electronic requirements and the  $\pi$ -acceptor and  $\pi$ -donor properties of the ligands bound to the metal center represent the driving force toward the selective formation of the mixed six-coordinated  $\text{M}^{\text{III}}\text{P}_2\text{S}_4$  arrangement, when a combination of

phosphinothiol and dithiocarbamate ligands coexists in the reaction mixture in the right stoichiometric ratio.

The opportunity to introduce a chemically different ligand after construction of the  $[\text{M}^{\text{III}}(\text{PS})_2]^+$  building block paves the way to the design of bidentate ligands conjugated to biomolecules such as pharmacophore groups, peptides, etc., for receptor targeting. In this perspective, dithiocarbamate ligands have shown to be of greatly useful in radiopharmaceutical design thanks to a wide variety of organic substituents that can be incorporated into the ligand backbone. This allows fine chemical modulation of the biological properties of the final complex by variation of the R substituent, independently of the other ligands on the metal.

If M–dithiocarbamate will prove to be kinetically stable in challenge reactions and in biological media, the possibility to easily insert this simply modifiable coligand into a mixed-ligand complex starting from permetalate anions will constitute the laying of the first stone for the preparation of a new series of  $\text{M}^{\text{III}}$ -based compounds useful in theragnostic applications. Studies are currently in progress in order to transfer this technology at the tracer level with  $^{99\text{m}}\text{Tc}$  and  $^{188}\text{Re}$ .

## ASSOCIATED CONTENT

### Supporting Information

Synthesis and characterization [elemental analysis, ESI(+)-MS, and IR spectroscopy] of the dinuclear  $\mu$ -oxorhenium(V)  $[\text{Re}_2\text{O}_3(\text{L})_4]$  complexes (L = L1–L4) along with that [elemental analysis, ESI(+)-MS, and  $^1\text{H}$  and  $^{13}\text{C}$  NMR spectroscopy] of EtOOCPIP2 and NaL3 ligands, ESI(+)-MS spectrum of complex **3** along with the proposed fragmentation, in accordance with a previously reported degradation mechanism of monoalkyl dithiocarbamates (Figure S1), NMR data of **9** (Figure S2–1–5), and crystallographic refinement details. This material is available free of charge via the Internet at <http://pubs.acs.org>. Crystallographic data for the structural analyses, in the form of CIF files, have been deposited with the Cambridge Crystallographic Data Centre as CCDC 912564 (1), CCDC 912565 (2), CCDC 912566 (7), and CCDC 912567 (9). These coordinates can be obtained, upon request, from the Director, Cambridge Crystallographic Data Centre, 12 Union Road, Cambridge CB2 1EZ, U.K. (e-mail [deposit@ccdc.cam.ac.uk](mailto:deposit@ccdc.cam.ac.uk) or [www:http://www.ccdc.cam.ac.uk](http://www.ccdc.cam.ac.uk)).

## AUTHOR INFORMATION

### Corresponding Author

\*E-mail: [bolzati@icis.cnr.it](mailto:bolzati@icis.cnr.it) (C.B.), [nicola.salvarese@unipd.it](mailto:nicola.salvarese@unipd.it) (N.S.). Phone: +39 049 8275352 (C.B.), +39 049 8275352 (N.S.). Fax: +39 049 8275366 (C.B.), +39 049 8275366 (N.S.).

### Notes

The authors declare no competing financial interest.

## ACKNOWLEDGMENTS

The authors thank Dr. Maria Grazia Ferlin for her helpful discussions, Dr. Daniele Dalzoppo and Dr. Fabio Maset for their support in mass spectrometric analysis, and Dr. Mariella Zancato for her work on elemental analysis. Special thanks are due to Dr. F. Benetollo of ICIS-CNR for the X-ray data collection for compound **7**. Financial support for the acquisition of the Oxford Diffraction/Agilent Gemini E diffractometer was provided by the University of Padova through the 2008 Scientific Equipment for Research initiative.

## REFERENCES

- (1) Bolzati, C.; Carta, D.; Salvarese, N.; Refosco, F. *Anti-Cancer Agents Med. Chem.* **2012**, *12*, 428–461.
- (2) Alberto, R.; Braband, H.; Can, D.; Tooyama, Y.; Imstepf, S. Technetium and Rhenium chemistry for radiopharmacy: quo vadis? In *Technetium and Other Metals in Chemistry and Medicine*; Mazzi, U., Eckelman, W. C., Volkert, W. A., Eds.; SGE. Ed. iali: Padova, Italy, 2010; pp 3–12.
- (3) Deutsch, E.; Vanderheyden, J.-L.; Gerundini, P.; Libson, K.; Hirth, W.; Colombo, F.; Savi, A.; Fazio, F. *J. Nucl. Med.* **1987**, *28*, 1870.
- (4) (a) Deutsch, E.; Bushong, W.; Glaven, K. A.; Elder, R. C.; Sodd, V. J.; Scholz, K. L.; Fortman, D. L.; Lukes, S. J. *Science* **1981**, *214*, 85. (b) Libson, K.; Barnett, B. L.; Deutsch, E. *Inorg. Chem.* **1983**, *22*, 1695. (c) Vanderheyden, J.-L.; Ketring, A. R.; Libson, K.; Heeg, M. J.; Roecker, L.; Motz, P.; Whittle, R.; Elder, R. C.; Deutsch, E. *Inorg. Chem.* **1984**, *23*, 3184. (d) Ichimura, A.; Heineman, W. R.; Vanderheyden, J.-L.; Deutsch, E. *Inorg. Chem.* **1984**, *23*, 1272. (e) Deutsch, E.; Ketring, A. R.; Libson, K.; Vanderheyden, J.-L.; Hirth, W. *Nucl. Med. Biol.* **1989**, *16*, 191. (f) Deutsch, E. *Radiochim. Acta* **1993**, *63*, 195.
- (5) (a) Pietzsch, H. J.; Spies, H.; Leibnitz, P.; Reck, G.; Berger, J.; Jacobi, R. *Polyhedron* **1992**, *11*, 1623. (b) Pietzsch, H. J.; Gupta, A.; Syhre, R.; Leibnitz, P.; Spies, H. *Bioconjugate Chem.* **2001**, *12*, 538. (c) Seifert, S.; Kunstler, J. U.; Schiller, E.; Pietzsch, H. J.; Pawelke, B.; Bergmann, R.; Spies, H. *Bioconjugate Chem.* **2004**, *15*, 856. (d) Schiller, E.; Seifert, S.; Tisato, F.; Refosco, F.; Kraus, W.; Spies, H.; Pietzsch, H. J. *Bioconjugate Chem.* **2005**, *16*, 634.
- (6) (a) Bandoli, G.; Mazzi, U.; Roncari, R.; Deutsch, E. *Coord. Chem. Rev.* **1982**, *44*, 191–227. (b) Tisato, F.; Refosco, F.; Bandoli, G. *Coord. Chem. Rev.* **1994**, *135/136*, 325–397. (c) Bandoli, G.; Dolmella, A.; Porchia, M.; Refosco, F.; Tisato, F. *Coord. Chem. Rev.* **2001**, *214*, 43–90. (d) Bandoli, G.; Dolmella, A.; Tisato, F.; Agostini, S. *Coord. Chem. Rev.* **2006**, *250*, 561–573.
- (7) (a) Mevellec, F.; Roucoux, A.; Noiret, N.; Patin, H.; Tisato, F.; Bandoli, G. *Inorg. Chem. Commun.* **1999**, *2*, 230–233. (b) Mevellec, F.; Tisato, F.; Refosco, F.; Roucoux, A.; Noiret, N.; Patin, H.; Bandoli, G. *Inorg. Chem.* **2002**, *41*, 598–601. (c) Lepareur, N.; Mevellec, F.; Noiret, N.; Refosco, F.; Tisato, F.; Porchia, M.; Bandoli, G. *Dalton Trans.* **2005**, 2866–2875.
- (8) Bolzati, C.; Refosco, F.; Tisato, F.; Bandoli, G.; Dolmella, A. *Inorg. Chim. Acta* **1992**, *7*–10.
- (9) Refosco, F.; Bolzati, C.; Moresco, A.; Bandoli, G.; Dolmella, A.; Mazzi, U.; Nicolini, M. *J. Chem. Soc., Dalton Trans.* **1991**, *11*, 3043–3048.
- (10) Tisato, F.; Refosco, F.; Bandoli, G.; Bolzati, C.; Moresco, A. *J. Chem. Soc., Dalton Trans.* **1994**, 1453–1461.
- (11) Maina, T.; Pecorale, A.; Dolmella, A.; Bandoli, G.; Mazzi, U. *J. Chem. Soc., Dalton Trans.* **1994**, *16*, 2437–2443.
- (12) Dilworth, J. R.; Griffiths, D. V.; Parrott, S. J.; Zheng, Y. *J. Chem. Soc., Dalton Trans.* **1997**, *17*, 2931–2936.
- (13) Rowbottom, J.; Wilkinson, G. *J. Chem. Soc., Dalton Trans.* **1972**, *7*, 826–830.
- (14) (a) Rouschias, G.; Wilkinson, G. *Inorg. Phys. Theor.* **1967**, 993–1000. (b) Archer, C. M.; Dilworth, J. R.; Thompson, R. M.; McPartlin, M.; Povey, D. C.; Kelly, J. D. *J. Chem. Soc., Dalton Trans.* **1993**, *3*, 461–466.
- (15) Bolzati, C.; Salvarese, N.; Carta, D.; Refosco, F.; Dolmella, A.; Pietzsch, H. J.; Bergmann, R.; Bandoli, G. *J. Biol. Inorg. Chem.* **2010**, *16*, 137–155.
- (16) North, A. T. C.; Philips, D. C.; Mathews, F. S. *Acta Crystallogr.* **1968**, *A24*, 351.
- (17) *CrysAlisPro*, version 1.171.33.52; Oxford Diffraction Ltd.: Abingdon, U.K. (release 06-11-2009 CrysAlis171.NET).
- (18) *CrysAlisPro*, version 1.171.35.15; Oxford Diffraction Ltd.: Abingdon, U.K. (release 03-08-2011 CrysAlis171.NET).
- (19) (a) Bolzati, C.; Refosco, F.; Tisato, F.; Bandoli, G.; Dolmella, A. *Inorg. Chim. Acta* **1992**, *201*, 7–10. (b) Bolzati, C.; Boschi, A.; Uccelli, L.; Malagò, E.; Bandoli, G.; Tisato, F.; Refosco, F.; Pasqualini, R.; Duatti, A. *Inorg. Chem.* **1999**, *38*, 4473–4479. (c) Bolzati, C.; Benini, E.; Cavazza-Ceccato, M.; Cazzola, E.; Malagò, E.; Agostini, S.; Tisato, F.; Refosco, F.; Bandoli, G. *Bioconjugate Chem.* **2006**, *17*, 419–428. (d) Bolzati, C.; Cavazza-Ceccato, M.; Agostini, S.; Tisato, F.; Bandoli, G. *Inorg. Chem.* **2008**, *47*, 11972–11983. (e) Bolzati, C.; Malagò, E.; Boschi, A.; Cagnolini, A.; Porchia, M.; Bandoli, G. *New J. Chem.* **1999**, *23*, 807–809.
- (20) Joris, S. J.; Aspila, K. I.; Chakrabarti, C. L. *Anal. Chem.* **1970**, *42*, 647–651.
- (21) Tolman, C. A. *Chem. Rev.* **1977**, *77*, 313–348.
- (22) Abram, U.; Lorenz, B.; Kaden, L.; Scheller, D. *Polyhedron* **1988**, *7*, 285–289.
- (23) Johnson, C. K. *ORTEP Report ORNL-5138*; Oak Ridge National Laboratory: Oak Ridge, TN, 1976.
- (24) *Mercury CSD 2.0—New Features for the Visualization and Investigation of Crystal Structures*; Macrae, C. F.; Bruno, I. J.; Chisholm, J. A.; Edgington, P. R.; McCabe, P.; Pidcock, E.; Rodriguez-Monge, L.; Taylor, R.; van de Streek, J.; Wood, P. A. *J. Appl. Crystallogr.* **2008**, *41*, 466.
- (25) (a) Shellenbarger-Jones, A.; Nicholson, T.; Davis, W. M.; Davison, A.; Jones, A. G. *Inorg. Chim. Acta* **2005**, *358*, 3559. (b) Dilworth, J. R.; Hutson, A. J.; Lewis, J. S.; Miller, J. R.; Zheng, Y.; Chen, Q.; Zubieta, J. *J. Chem. Soc., Dalton Trans.* **1996**, 1093.
- (26) (a) Kannan, R.; Pillarsetty, N.; Gali, H.; Hoffman, T. J.; Barnes, C. L.; Jurisson, S. S.; Smith, C. J.; Volkert, W. A. *Inorg. Chem.* **2011**, *60*, 6210. (b) Smith, C. J.; Katti, K. V.; Volkert, W. A.; Barbour, L. J. *Inorg. Chem.* **1997**, *36*, 3928.
- (27) Tisato, F.; Refosco, F.; Porchia, M.; Bolzati, C.; Bandoli, G.; Dolmella, A.; Duatti, A.; Boschi, A.; Jung, C. M.; Pietzsch, H.-J.; Kraus, W. *Inorg. Chem.* **2004**, *43*, 8617.
- (28) Allen, F. H. *Acta Crystallogr.* **2002**, *B58*, 380. Cambridge Structural Database (version 5.33 of Nov 2011 + 2 updates).